

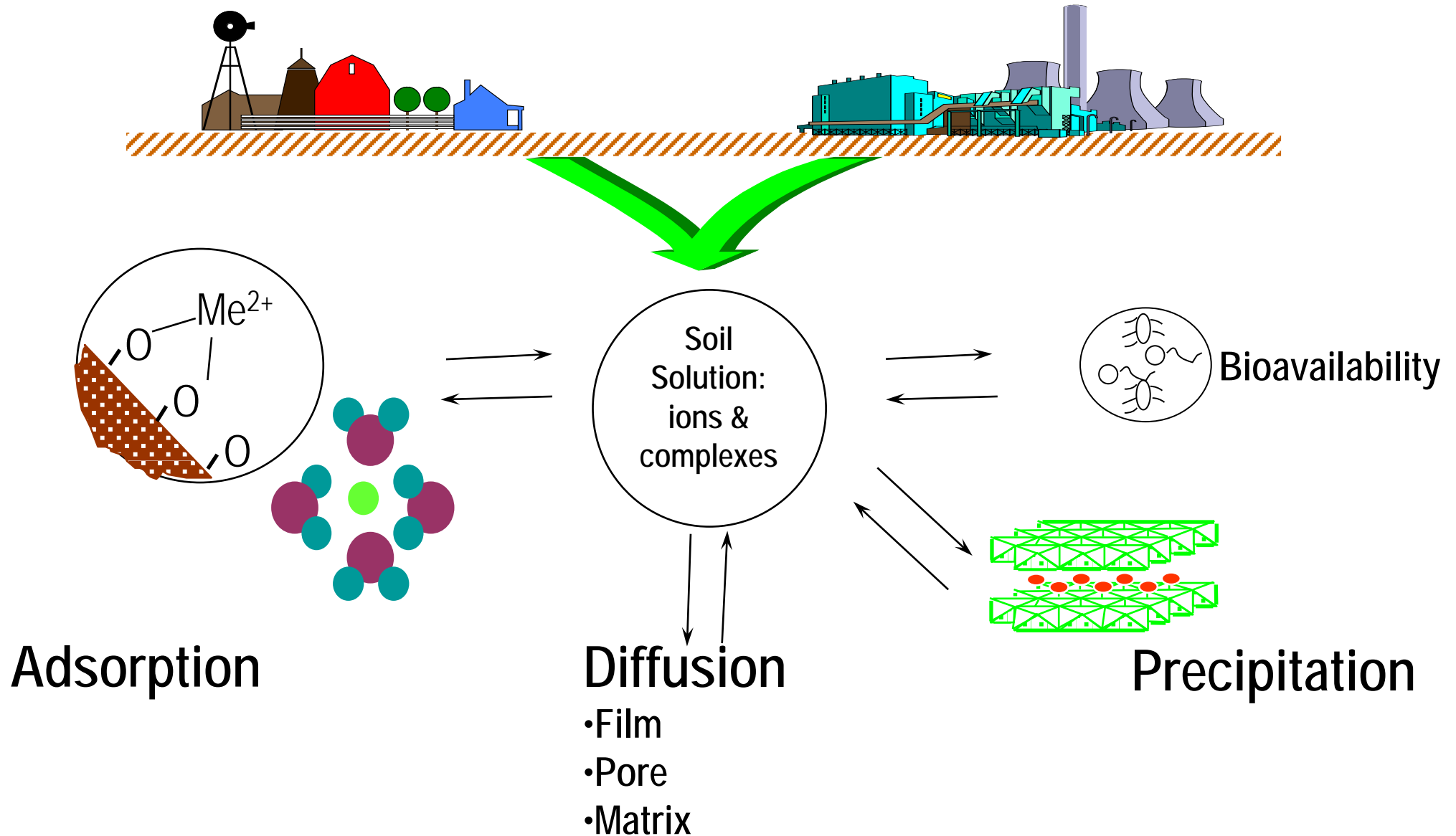


Wir schaffen Wissen – heute für morgen

# Introduction to EXAFS practical – scientific problem to be analysed

Camelia Borca  
Paul Scherrer Institute

# Introduction of Metals into Soil Environments: Primary minerals, Agriculture, Industry, Sewage sludge, etc



- Iron (Fe) - abundant in earth crust, mostly as iron (hydr)oxides
- 16 different (hydr)oxides, mostly formed as weathering products
- Often nano-sized crystals with high surface area – most reactive sorbents for contaminants in the environment



# We will look at the structure of:

## Ferrihydrite

Very common iron hydroxide

Poorly ordered

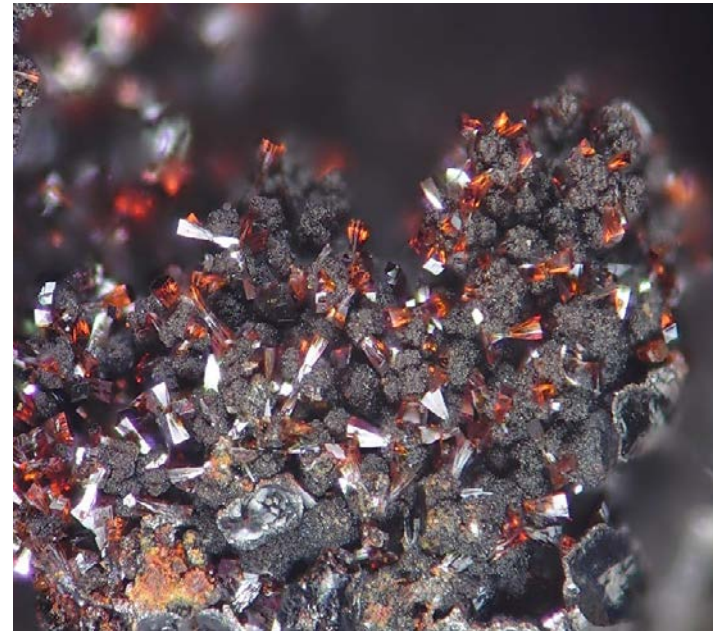
Structure/chemical formula unclear



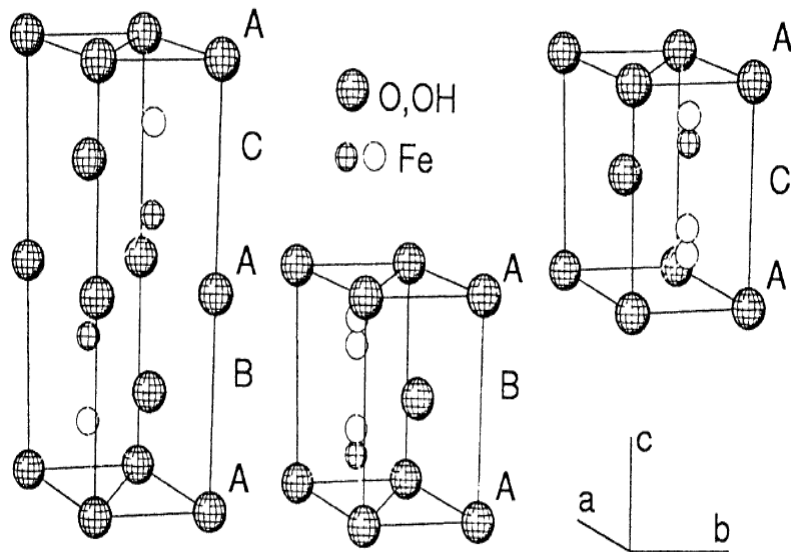
## Lepidocrocite

Orthorhombic crystal structure

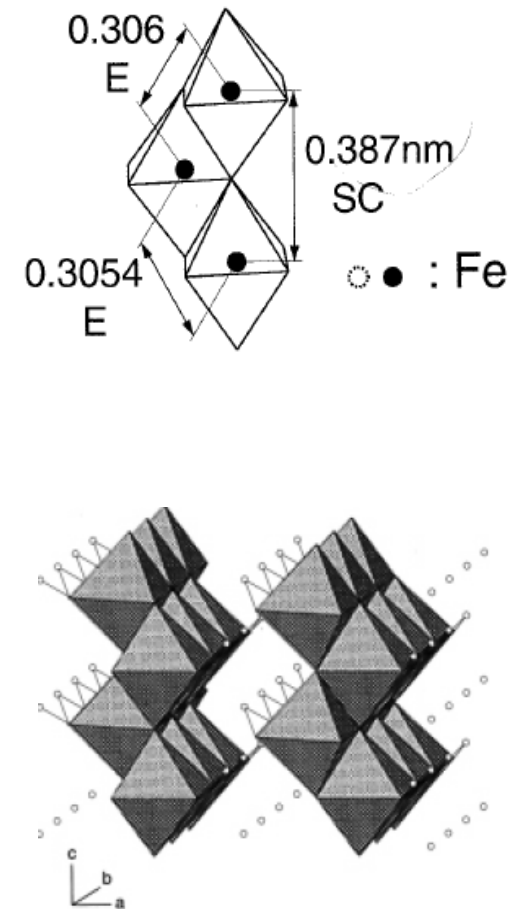
Well-crystalized



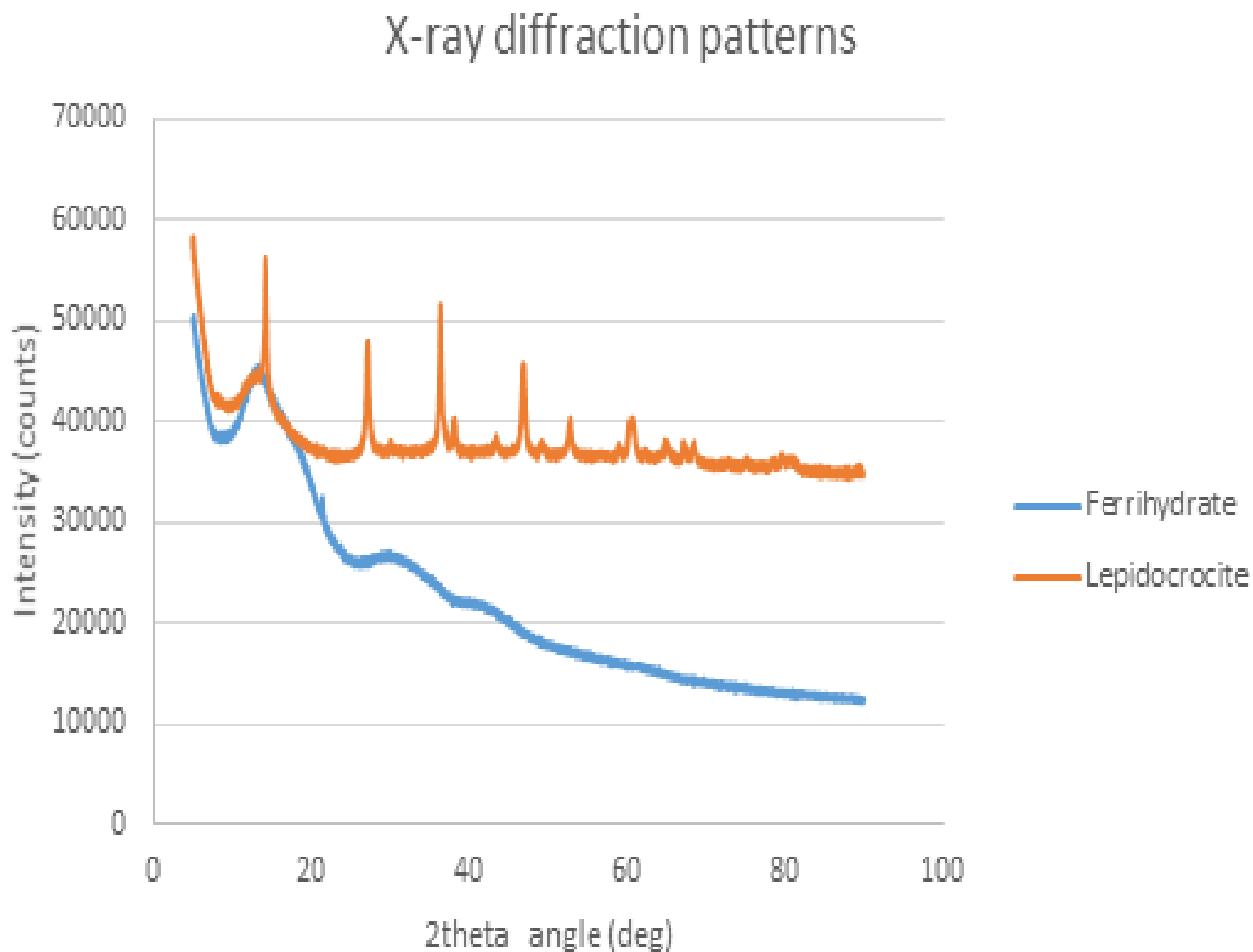
## Ferrihydrite $\text{Fe}_5\text{O}_8\text{H}\cdot 4\text{H}_2\text{O}(?)$



## Lepidocrocite ( $\gamma\text{-FeOOH}$ )



# But.... Do we know the structure? .... XRD



and by the curvature coupling of stretching ions to the reaction coordinate (26–28), i.e., a bifurcation of reaction paths for stretched reactants must occur, presumably near the transition state. The normal branching fraction for the nonadiabatic pathway is quite substantial,  $\alpha_1^2/(\alpha_1^2 + \alpha_2^2) \sim 0.5$  from Fig. 3 (where  $\alpha_1^2$  and  $\alpha_2^2$  are the parabolic cross sections for the (0,0) and (1,0) last pairs from the stretch-excited reaction, actively), indicating a facile process. Theory predicts a strong Curio's coupling between stretching and bending modes (20, 27); this is nonadiabatic transition could then be aided and facilitated by the transitional nature of bending motions of the CD, vicinity during course of the reaction.

**References and Notes**  
1. C. Fabry, *Acc. Chem. Res.* **5**, 161 (1972).  
2. N. Zare, *Science* **279**, 1875 (1998).  
3. F. C. C. Chen, *Acc. Chem. Res.* **32**, 877 (1999).  
4. K. Liu, *J. Chem. Phys.* **125**, 11210F (2006).  
5. K. Liu, *Phys. Chem. Chem. Phys.* **9**, 17 (2007).  
6. S. Yuan, S. Herten, A. N. Zolotarev, F. F. Crim, *J. Chem. Phys.* **116**, 10744 (2002).  
7. S. Yuan, R. J. Hilday, F. F. Crim, *J. Chem. Phys.* **119**, 4955 (2003).  
8. S. Yuan, R. J. Hilday, T. L. Sherrill, F. F. Crim, *J. Chem. Phys.* **119**, 9968 (2003).  
9. R. J. Hilday, C. H. Nien, C. J. Anzures, F. F. Crim, *J. Chem. Phys.* **125**, 131101 (2006).  
10. M. R. Stoper, T. P. Raitis, S. A. Kanicki, T. L. Sherrill, N. Zare, *J. Phys. Chem.* **100**, 7938 (1996).

## The Structure of Ferrihydrite, a Nanocrystalline Material

F. Marc Michel,<sup>1,2\*</sup> Lars Elm,<sup>1,2</sup> Sylie M. Antao,<sup>3</sup> Peter L. Lee,<sup>4</sup> Peter J. Chupas,<sup>4</sup> Gang Liu,<sup>1,4</sup> Daniel R. Strongin,<sup>1,4</sup> Martin A. A. Schoone,<sup>1,2</sup> Brian L. Phillips,<sup>1,2</sup> John B. Parise<sup>1,2,3</sup>

Despite the ubiquity of ferrihydrite in natural sediments and its importance as an industrial sorbent, the nanocrystallinity of this iron oxyhydroxide has hampered accurate structure determination by traditional methods that rely on long-range order. We uncovered the atomic arrangement by real-space modeling of the pair distribution function (PDF) derived from direct Fourier transformation of the total x-ray scattering. The PDF for ferrihydrite synthesized with the use of different routes is consistent with a single phase (hexagonal space group  $P6_3mc$ ;  $a = 5.935$  angstroms,  $c = 9.06$  angstrom). In its ideal form, this structure contains 20% tetrahedrally and 80% octahedrally coordinated iron and has a basic structure. Real-space fitting indicates structural second-order effects such as internal

Ferrihydrite is ubiquitous in surface environments (1, 2) and is widely used in industrial applications (3, 4). It occurs in pristine soil as the precursor to hematite as a result of acid mine drainage. Because of its extremely high surface reactivity, ferrihydrite plays a substrate

### CRYSTAL GROWTH

## Aqueous formation and manipulation of the iron-oxo Keggin ion

Omid Sadeghi, Lev N. Zakharov, May Nyman\*

There is emerging evidence that growth of synthetic and natural phases occurs by the aggregation of prenucleation clusters, rather than classical atom-by-atom growth. Ferrihydrite, an iron oxyhydroxide mineral, is the common form of  $Fe^{3+}$  in soils and is also in the ferritin protein. We isolated a 10 angstrom diameter iron-oxo cluster (known as the Keggin ion,  $Fe_{13}$ ) that has the same structural features as ferrihydrite. The stabilization and manipulation of this highly reactive polyanion in water is controlled exclusively by its counterions. Upon dissolution of  $Fe_{13}$  in water with precipitation of its protecting  $Bi^{3+}$  counterions, it rapidly aggregates to ~22 angstrom spherical ferrihydrite nanoparticles.  $Fe_{13}$  may therefore also be a prenucleation cluster for ferrihydrite formation in natural systems, including by microbial and cellular processes.

Iron oxides and oxyhydroxides are ubiquitous in the environment and serve vital roles in interrelated phenomena of contaminant transport, pH control of surface and ground water, and microbial activity (1–4). Relevant phases include hematite, magnetite, goethite, and ferrihydrite. The structure of ferrihydrite,

the most common iron oxyhydroxide in soil and in the core of the ferritin protein, is intractable to the Al-mineral solubility (5). The ferrihydrite structure has been highly debated (6–8), but the general framework contains linked and faced iron-oxyhydroxide Keggin units. The Keggin ion or molecule is a metal-oxo structural motif in natural and synthetic materials (9). Even before the proposed structure of ferrihydrite, an iron Keggin cluster (henceforth referred to as  $Fe_{13}$ ) was proposed to be synthetically stabilizable—analogueous to

Oregon State University, Department of Chemistry, Corvallis, OR 97331, USA.  
\*Corresponding author. Email: may.nyman@oregonstate.edu

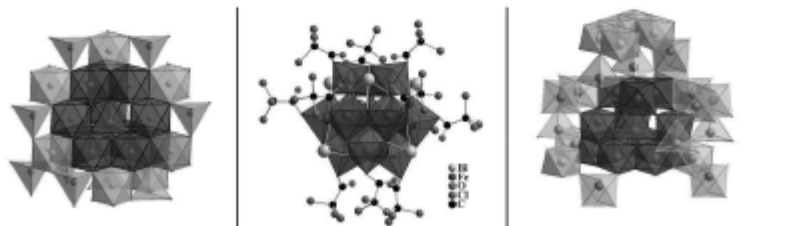


**Fig. 1. The iron Keggin ion.** Views of the iron Keggin ion in different structures. (Left) Magnetite,  $(Fe^{2+}_{12}Fe^{3+}_{12})_2O_4$  emphasizing the  $Fe_{13}$  Keggin building unit (red polyhedra). The four trimers of edge-sharing octahedra are likewise connected together by edge-sharing. (Middle)  $Bi_4(Fe_{13}O_{12}O_2(OH)_2(O_2O)(CO_3)_2)P^{3-}$ .  $Bi_4Fe_{13}O_{12}$  in the  $\alpha$ -isomer, the four trimers are linked together by corner-sharing. (Right) A view of ferrihydrite, structure determined from pair distribution function (5). The red polyhedra emphasize the  $Fe_{13}$  building block. In the  $\alpha$ -isomer, three of the trimers are edge-sharing, and the fourth is corner-linked.

## Size-Driven Structural and Thermodynamic Complexity in Iron Oxides

Alexandra Navrotsky,<sup>1\*</sup> Lena Mazela,<sup>2</sup> Jura Majtan<sup>3</sup>

Iron oxides occur ubiquitously in environmental, geological, planetary, and technological settings. They exist in a rich variety of structures and hydration states. They are commonly fine-grained (nanophase) and poorly crystalline. This review summarizes recently measured thermodynamic data on their formation and surface energies. These data are essential for calculating the thermodynamic stability fields of the various iron oxide and oxyhydroxide phases and understanding their occurrence in natural and anthropogenic environments. The competition between surface enthalpy and the energetics of phase transformation leads to the general counter-intuitive observation that smaller crystals can often be

more stable than larger crystals can often be in oxides in nature.

The identified nonclassical growth behavior of iron oxides in both nature (3) and the laboratory (2)—defined by the aggregation of prenucleation clusters rather than atom-by-atom growth—supports the existence of a discrete  $Fe_{13}$  ion as a precursor to ferrihydrite and magnetite (Fig. 1). However, the higher reactivity (acidity) of  $Fe^{3+}$ -bound  $H_2O$  as compared with  $Al^{3+}$ -bound  $H_2O$  in the  $Al_3$  Keggin ion has thus far thwarted all synthetic efforts to capture a discrete  $Fe_{13}$  ion from water. Instead, iron oxyhydroxide nanoparticles and precipitates are obtained, bypassing the intermediate discrete cluster state. The closest species to  $Fe_{13}$  reported thus far is  $[FeO_4Fe_9(OCH_3)_3]^{3-}$  (3). Although possessing the Keggin structure, this cluster was synthesized in anhydrous conditions and is surface-passivated entirely with nonaqueous ligands. It is neither a truly precursor for iron oxide nucleation, nor provides identification of the aqueous ligand and ion-charge of  $Fe_{13}$  derived from water.

Here, we present strategies to stabilize and crystallize the discrete  $Fe_{13}$  Keggin ion from water and redissolve it in water, both as unassociated and aggregated forms. Because  $Fe_{13}$  is a very highly charged polyanion, contrary to the analogous  $Al_3$  polyanion, we chose likewise highly charged counterions ( $Bi^{3+}$ )

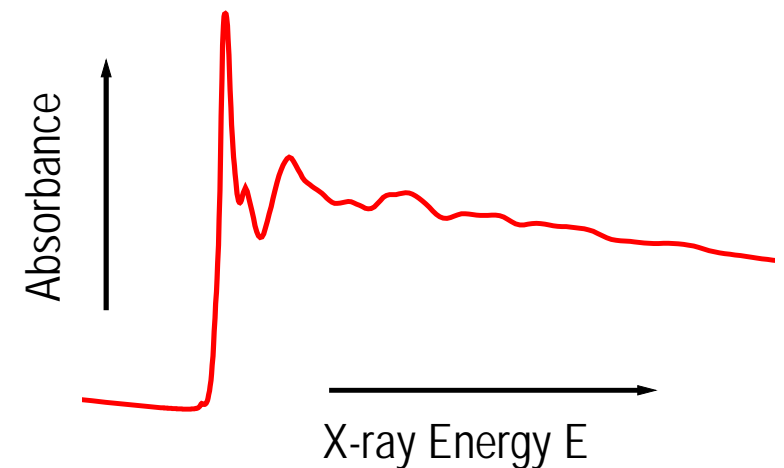
of iron as a nutrient. They have many commercial applications: pigments, catalysis, medical devices, sensors, and recording media. Nanotechnology increasingly makes use of iron oxide nanoparticles and thin films. Iron oxides exist in a bewildering variety of polymorphs (7). Anhydrous iron oxides include hematite ( $\alpha-Fe_2O_3$ ), magnetite ( $\gamma-Fe_2O_3$ ), and the less common  $\delta$ - and  $\beta-Fe_2O_3$  (mag-

netite) and  $Fe_3O_4$  (wüstite) contain both ferric and ferrous iron. Magnetite and maghemite, both spinels, can form a continuous solid solution. The oxyhydroxides, nominally  $Fe(OH)_3$ , include goethite, lepidocrocite, akaganeite, and several other polymorphs. They often contain excess water. More hydrated forms such as ferrihydrite, nominally  $Fe(OH)_3$ , have even more variable water content. Hydrated phases containing both ferrous and ferric iron include the green rust, layered hydroxides with different anions in the interlayer. A further complication is that many iron oxides, both in nature and in the laboratory, are exceedingly fine-grained (nanophase) and therefore hard to characterize.

This complexity has meant that until recently, knowledge of the structural details, thermodynamics, and reactivity of iron oxides has been lacking. One could not understand or predict which phases form under what conditions, and polymorphs are stable and which metastable, and

$S^\circ$ (J mol <sup>-1</sup> K <sup>-1</sup> )	$\Delta S_f^\circ$ (J mol <sup>-1</sup> K <sup>-1</sup> )	$\Delta G_f^\circ$ (kJ mol <sup>-1</sup> )	$\Delta H_f^\circ$ (J mol <sup>-1</sup> )	$\Delta H_f^\circ$ (J mol <sup>-1</sup> )
87.4 ± 0.2 (3)	-274.5 ± 0.3 (3)	-744.4 ± 1.3 (3)	0.75 ± 0.16 (13)	1.9 ± 0.3 (18)
93.0 ± 0.2 (17)	-268.9 ± 0.3 (17)	-731.4 ± 2.0	0.57 ± 0.10 (4)	0.71 ± 0.13 (8)
		-717.8 ± 6.6 (15)		
59.7 ± 0.2 (17)	-237.9 ± 0.2 (17)	-490.6 ± 1.5	0.60 ± 0.10 (12)	0.91 ± 0.09 (8)
65.1 ± 0.2 (17)	-232.5 ± 0.2 (17)	-482.7 ± 3.1	0.40 ± 0.16 (16)	0.62 ± 0.14 (8)
53.8 ± 3.3 (3)	-246.2 ± 3.3 (3)	-481.7 ± 1.9	0.34 ± 0.04 (11)	0.44 ± 0.04 (11)
		-483.1 ± 1.3 (13)		
		-711.0 ± 2.0 (15)		

- ✓ Detailed chemical and structural information (oxidation state, coordination numbers, bond distances, system disorder)
  - Solution species
  - Crystalline and amorphous solids
  - Surface complexes
- ✓ in-situ, non-destructive
- ✓ minimal sample preparation
- ✓ high selectivity/sensitivity (few ppm)





# X-ray absorption spectroscopy

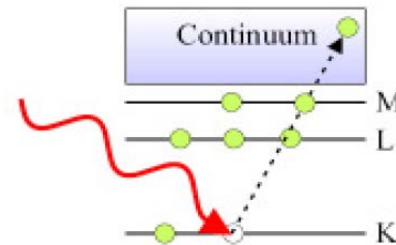
Visible light  
 $\lambda \sim 0.5 \mu\text{m}$   
 $E \sim 2 \text{ eV}$



X-ray light  
 $\lambda \sim 1 \text{ \AA} (=0.1 \text{ nm})$   
 $E \sim 10 \text{ keV}$



valence  
electrons

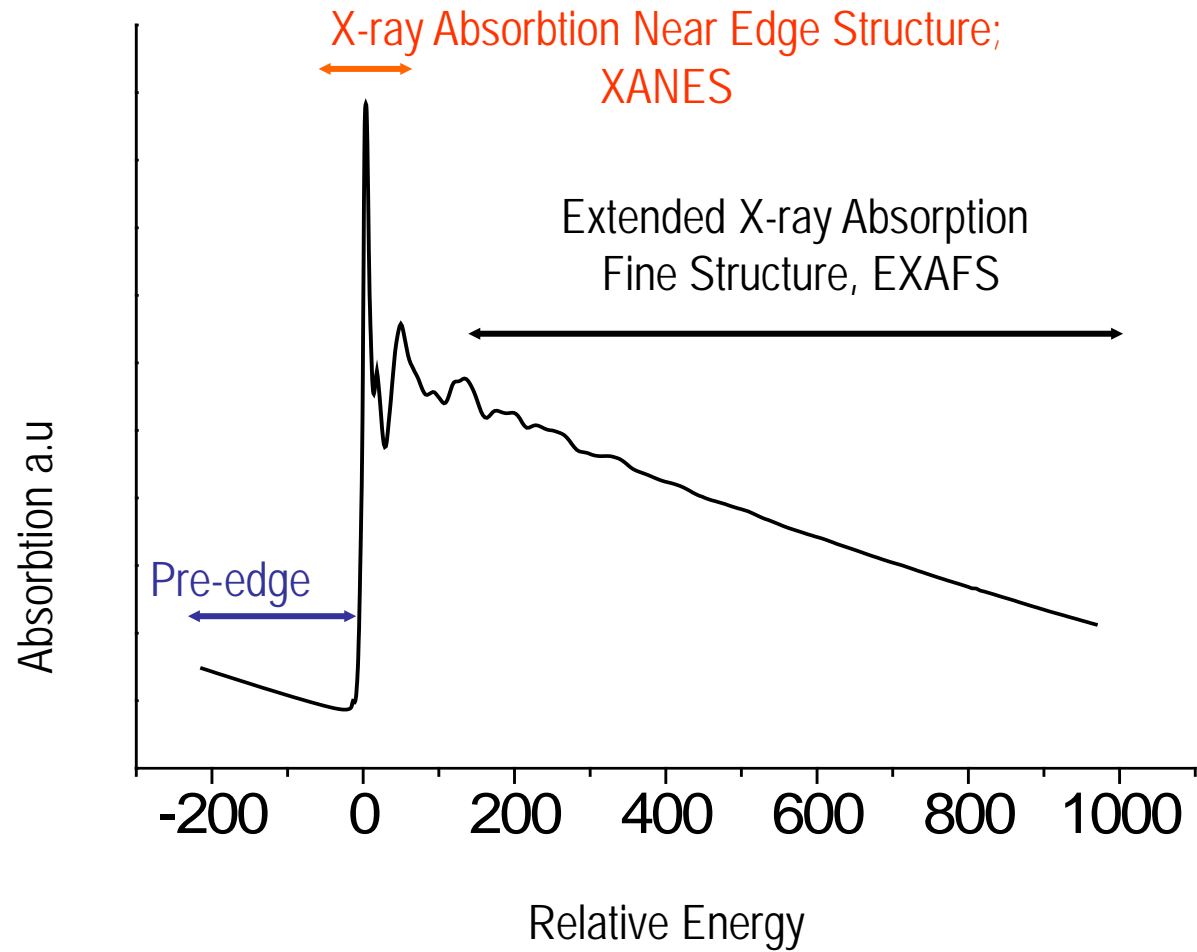
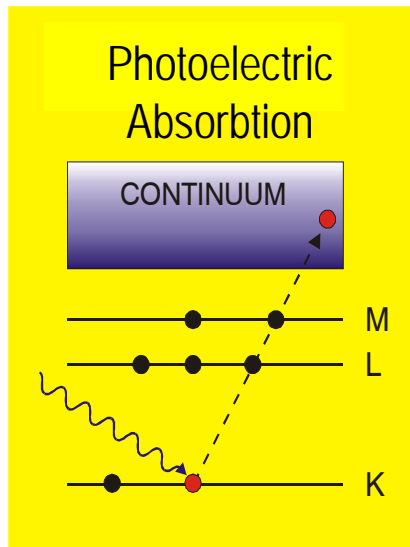


core  
electrons

Energy ↑



# Main Principle



- $E < E_b$
- transition of  $e^-$  from ground state (e.g.,  $1s, 2s$ ) to empty or partly filled, excited states ( $nd$  orbital)

- selection rules for  $e^-$  transitions

- speciation of Cr(VI) and Cr(III)

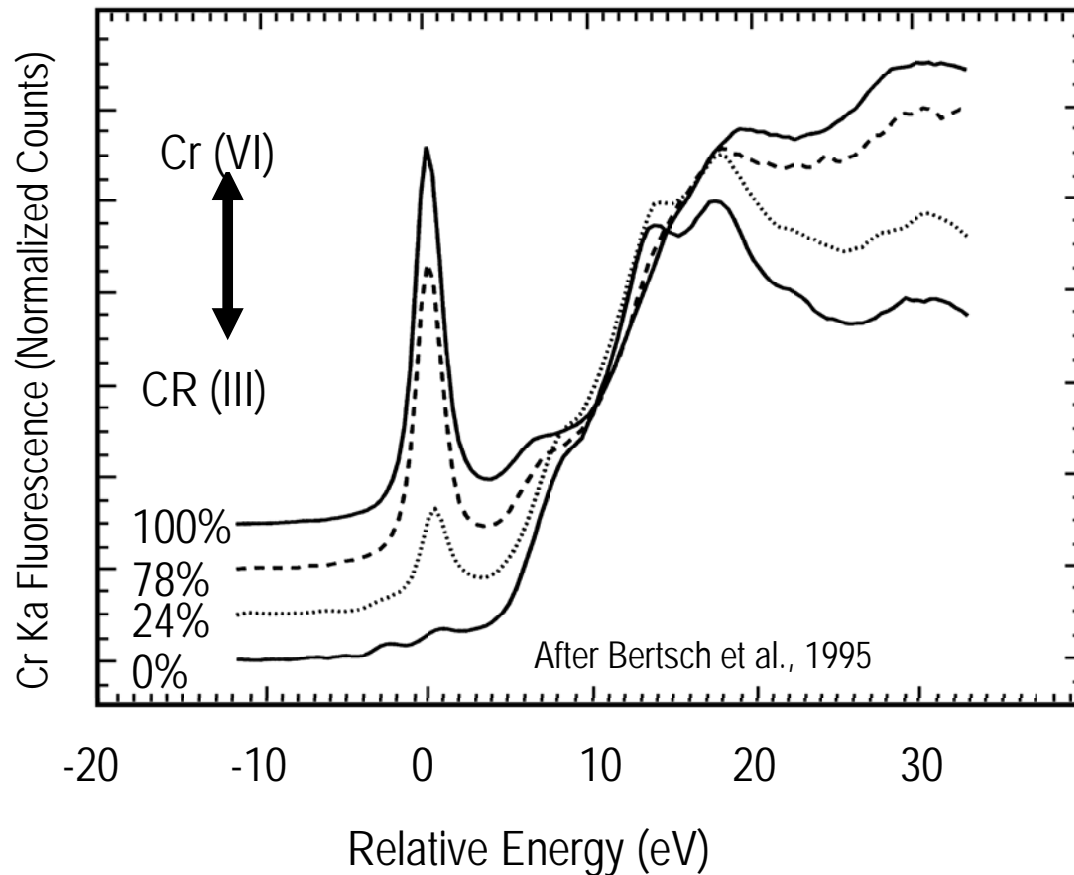
- Cr(VI)

- toxic and mobil

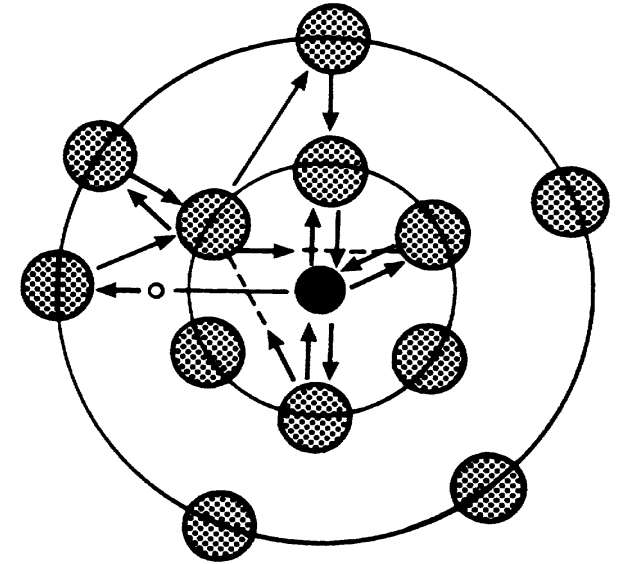
- Cr(III)

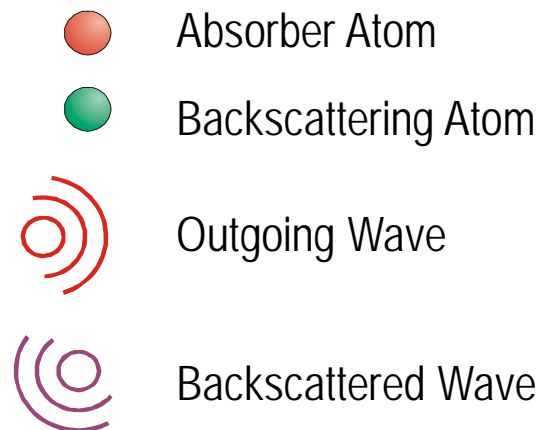
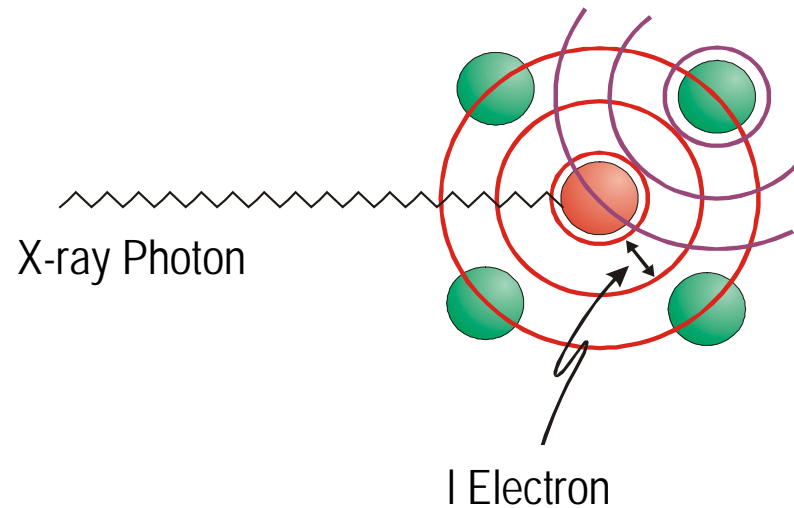
- hardly toxic

- sorbed or incorporated into mineral phases



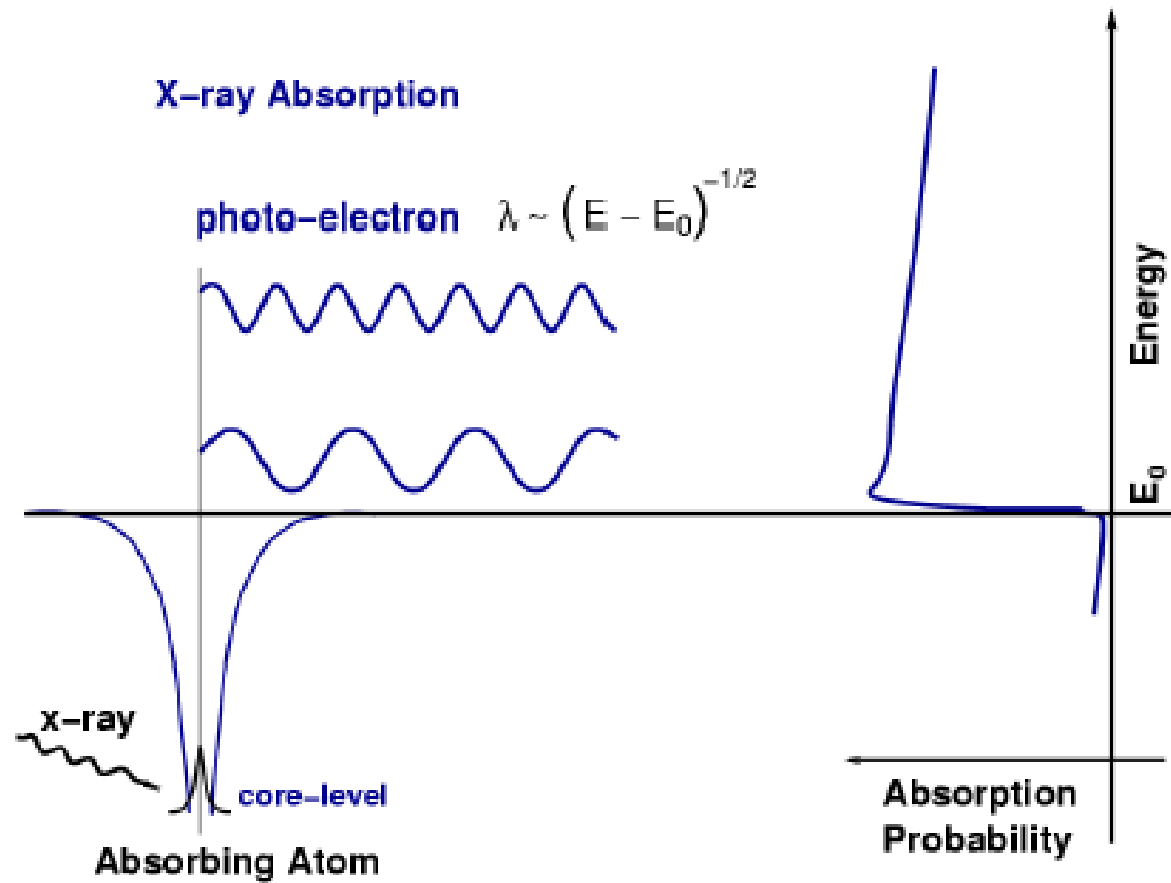
- $E \sim E_b$
- Multiple scattering of photoelectron
- Very intense and complicate resonance features: fingerprinting and theoretial calculations
- Energy of absorption edge depends on oxidation state
  - o Chemical shift of 1-3 eV for each withdrawing  $e^-$



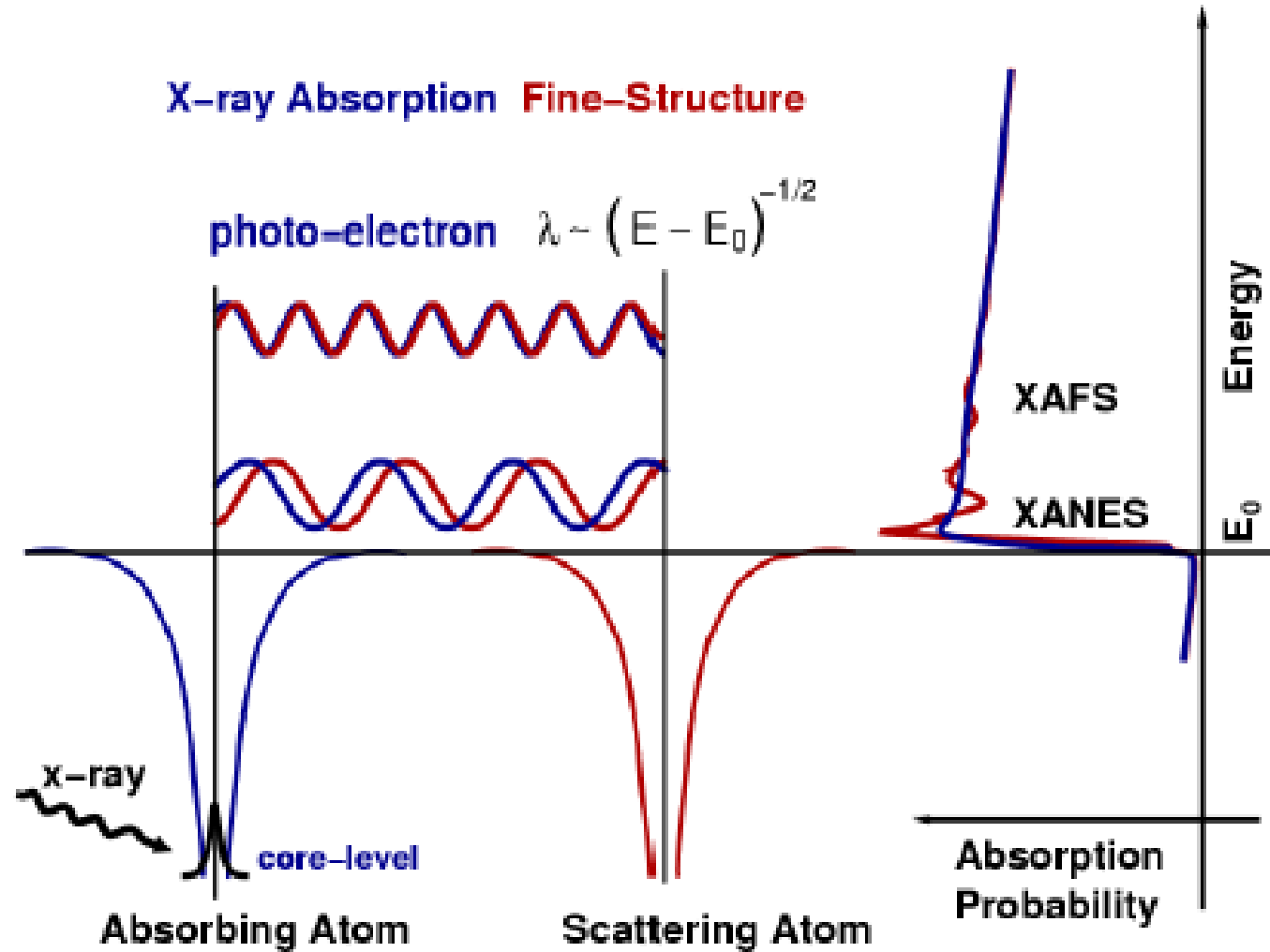


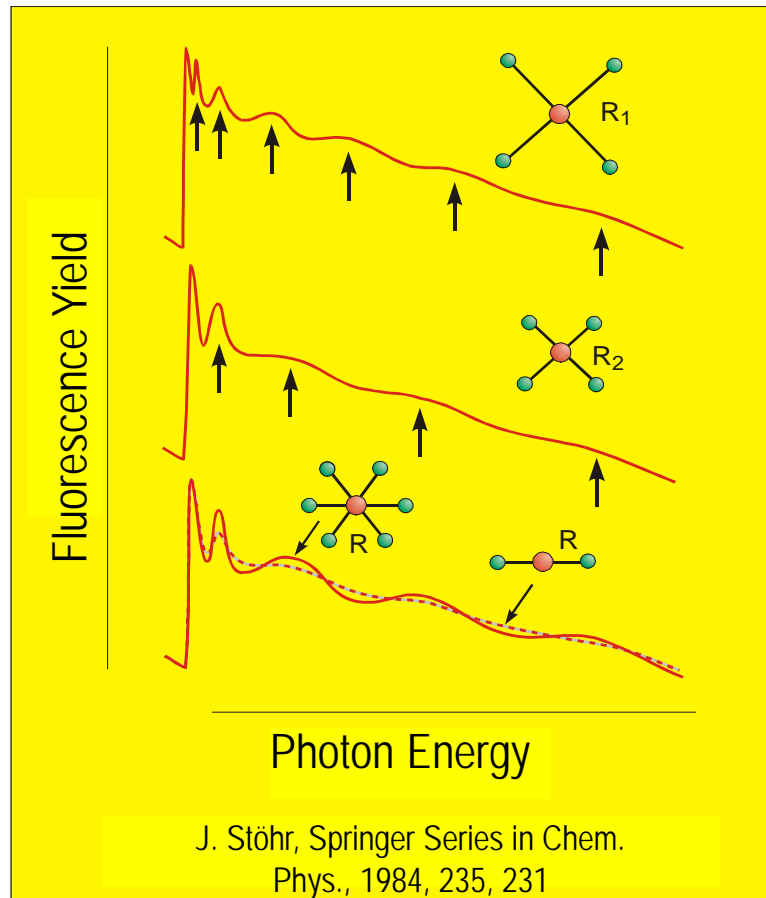
- $E > E_b$
- 50 - 1000 eV above absorption edge
- simplified illustration: constructive & destructive frequencies from the outgoing photoelectron

## Free atom



# Cluster of atoms



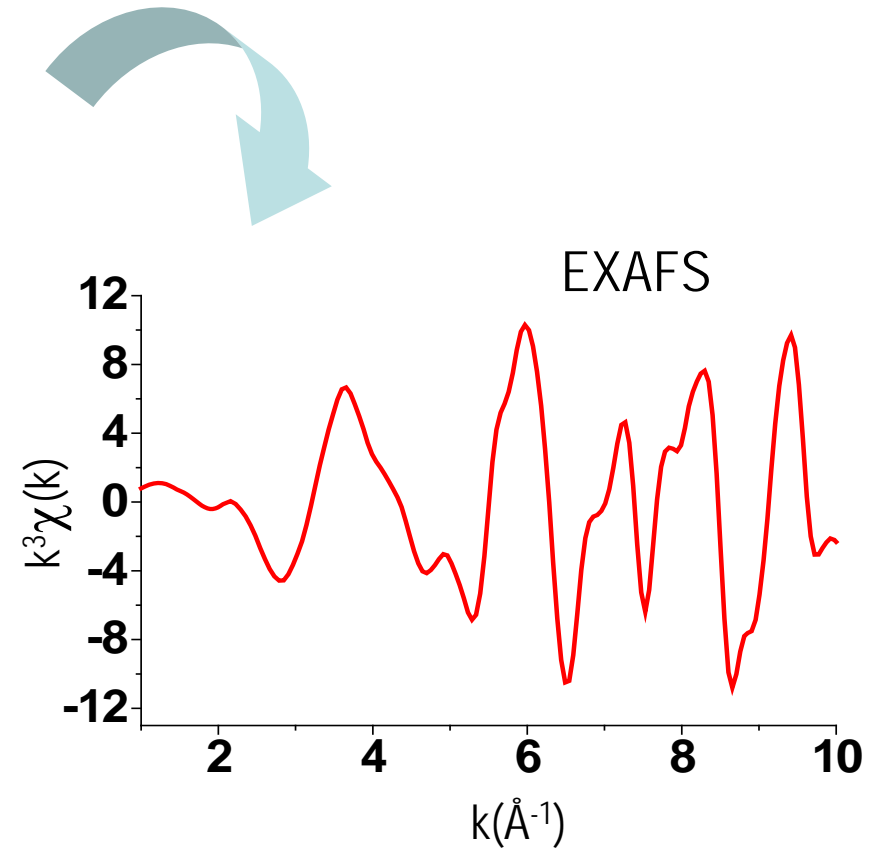
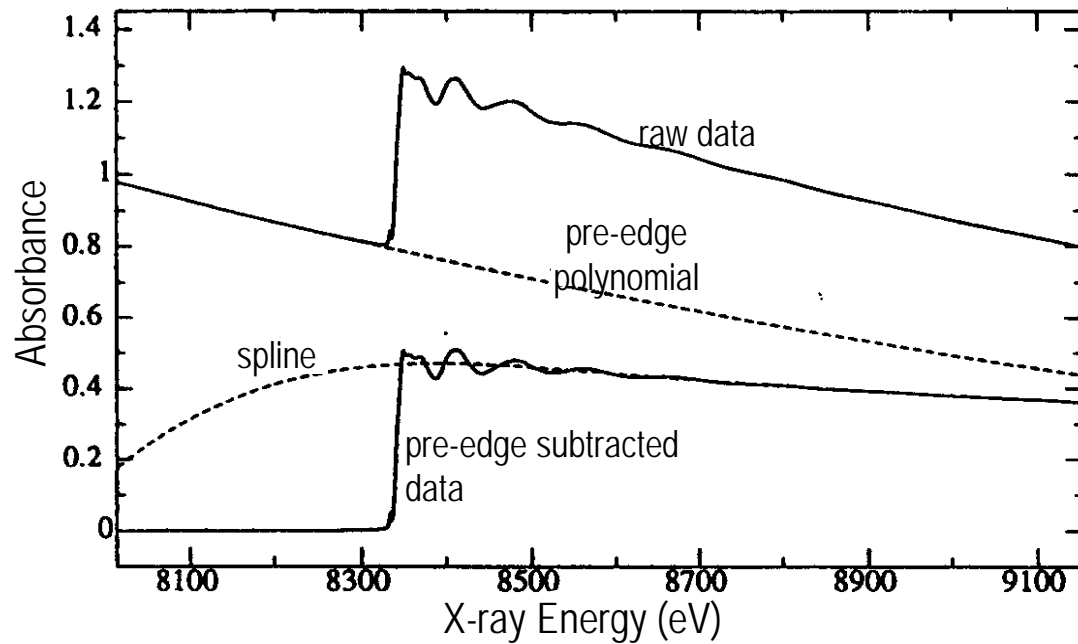


➤ Interference pattern (EXAFS)

- Frequency correlated to bond distance
- Amplitude correlated to coordination number and identity

$$\chi(k) = \sum a(k) \sin[2kR + \alpha(k)]$$

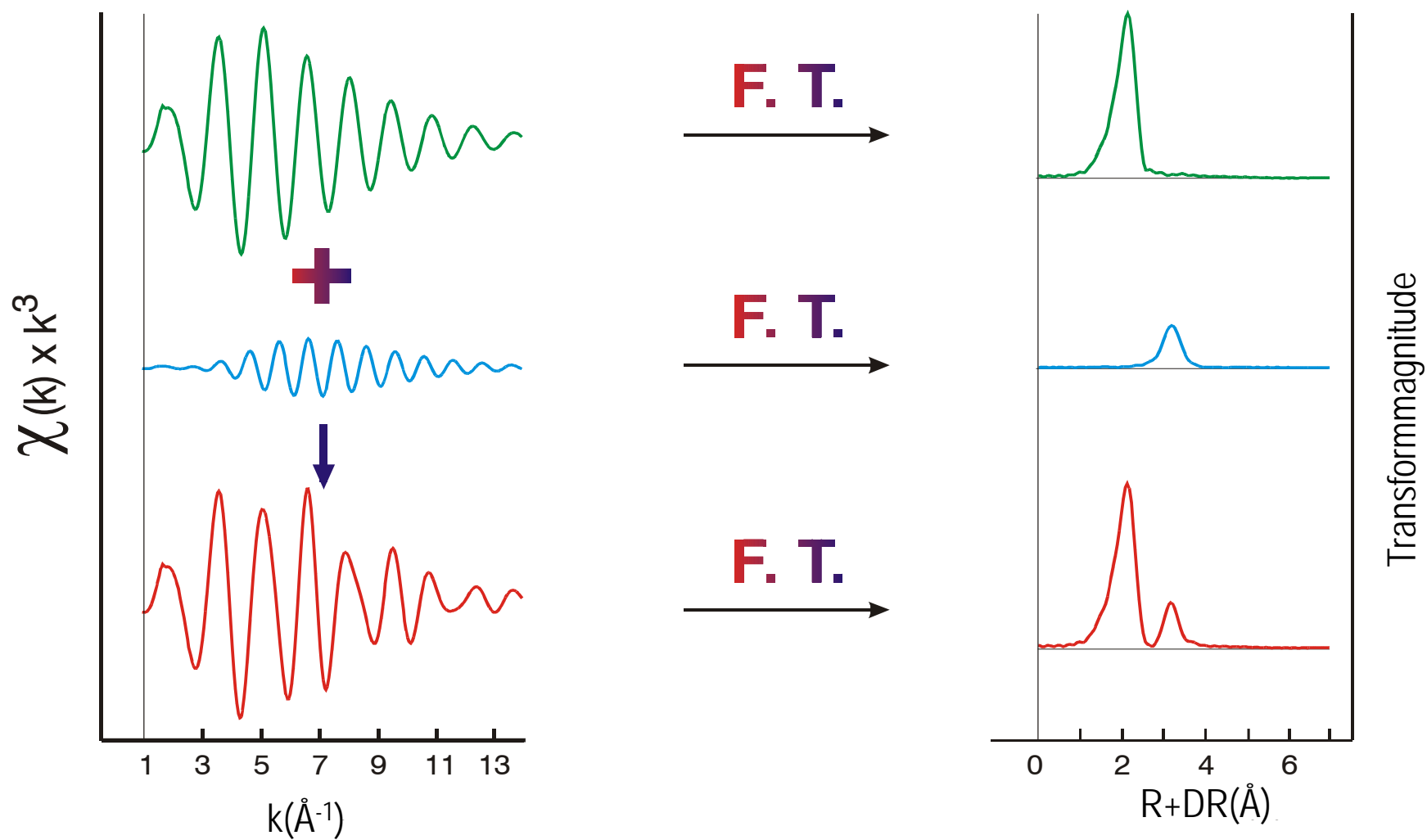




## ➤ extraction of EXAFS

- pre-edge & spline, normalization
- conversion to wave vector  $k^2 = 2m (E - E_0) / \hbar^2$
- normally weighted by  $k^3$

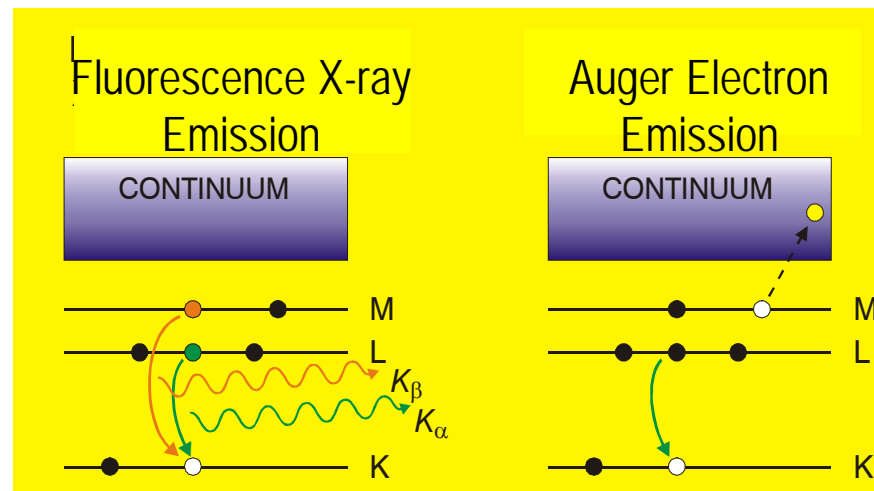
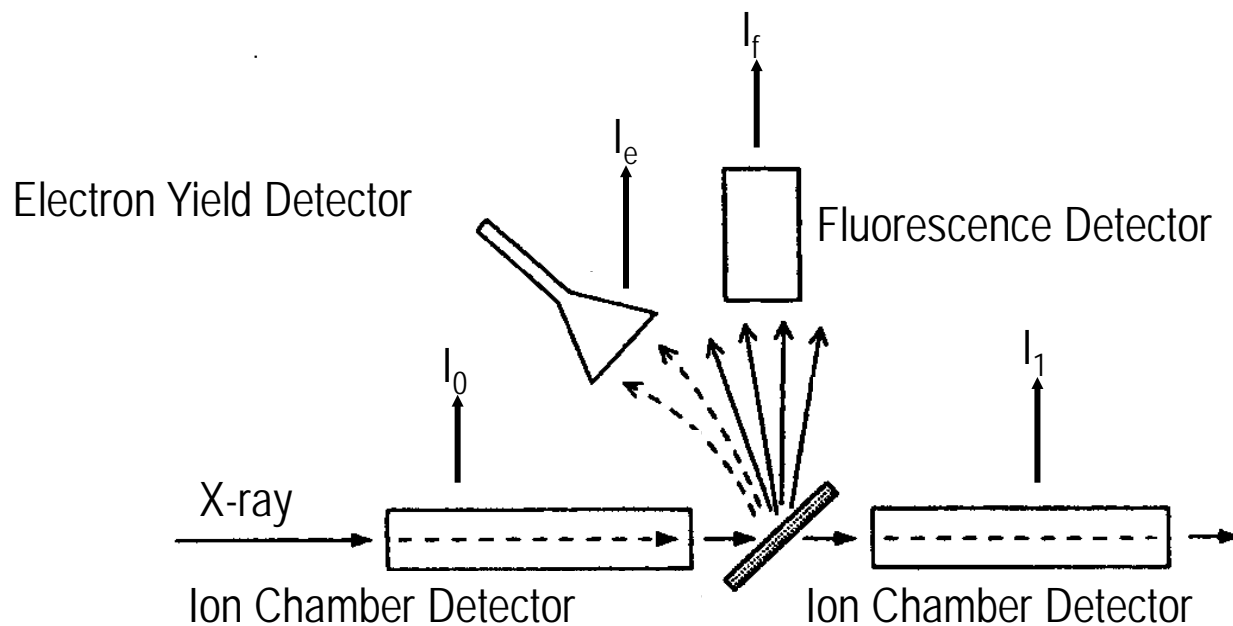
## Fourier Transformation

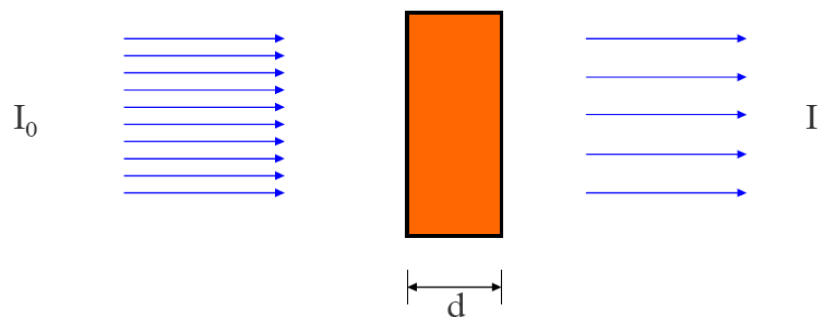


$$\chi(k) = \sum a(k) \sin[2kR + \alpha(k)]$$

# Experimental set-up

- Transmission
  - $A = mx = \ln(I_0/I_1)$
  - concentrated samples
- Fluorescence
  - $A = mx = I_f/I_0$
  - dilute samples
- Electron-yield
  - $A = mx = I_e/I_0$
  - surface sensitive

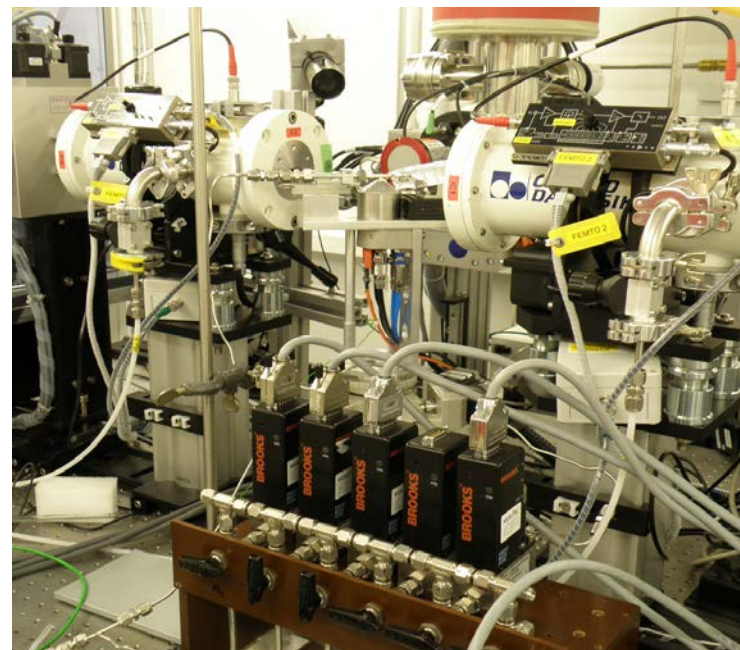




Lambert Beer's Law:  $I = I_0 \cdot e^{-\mu d}$

$\mu$  depends strongly on x-ray energy  $E$  and atomic number  $Z$ , and on the density  $\rho$  and Atomic mass  $A$ :

$$\mu \approx \frac{\rho Z^4}{A E^3}$$



What do you measure?

- Absorption as function of energy

# Need a Synchrotron...

SLS



Diamond



Soleil

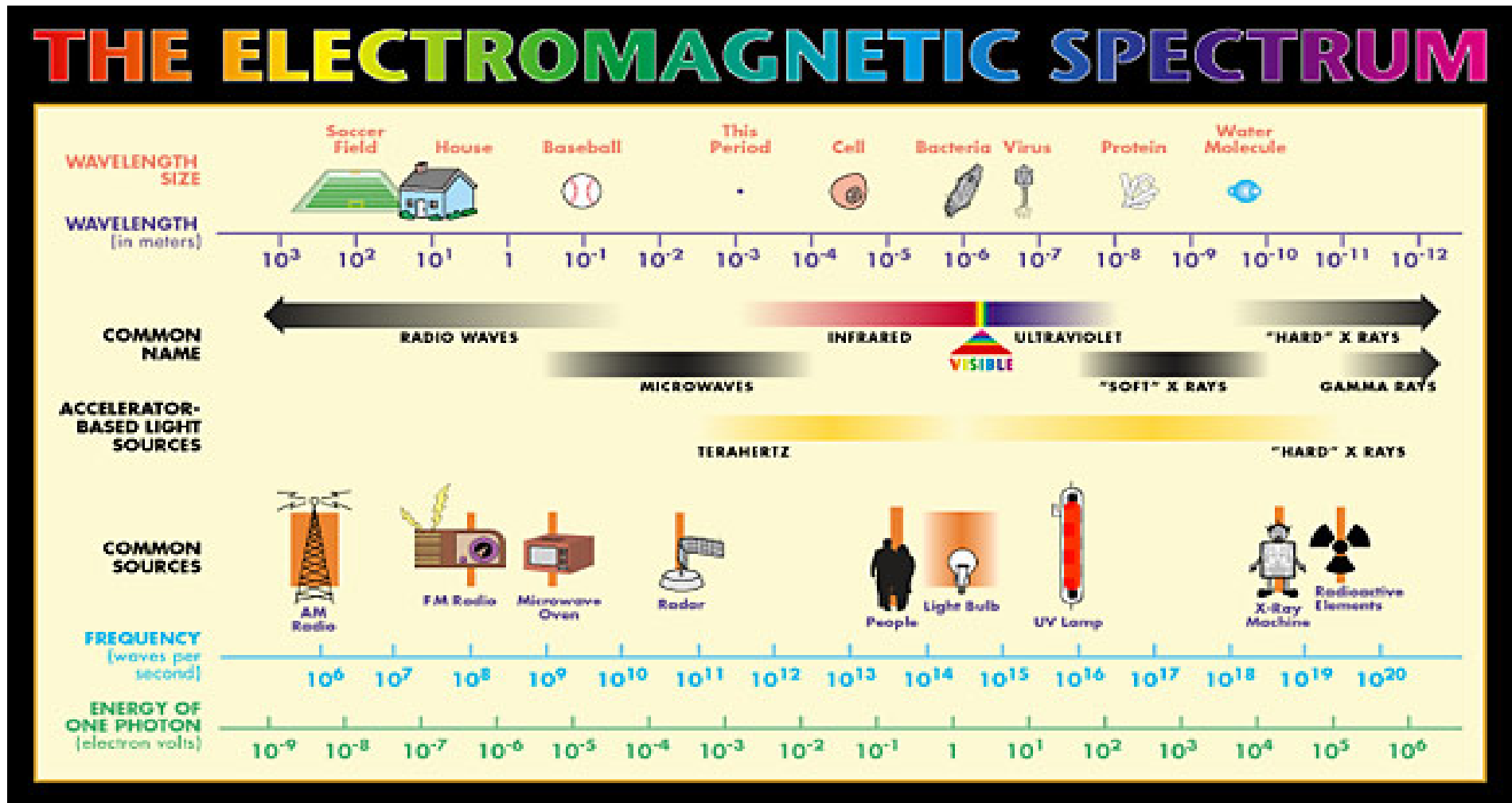


ESRF

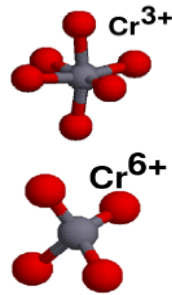
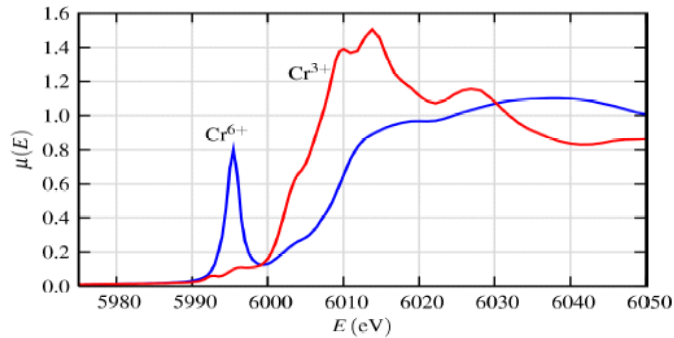


and many more...

# Synchrotrons produce **bright** light

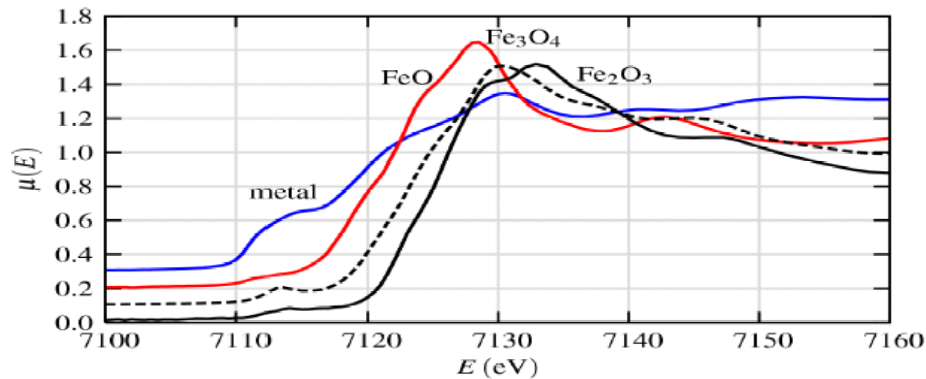


# Summary so far:



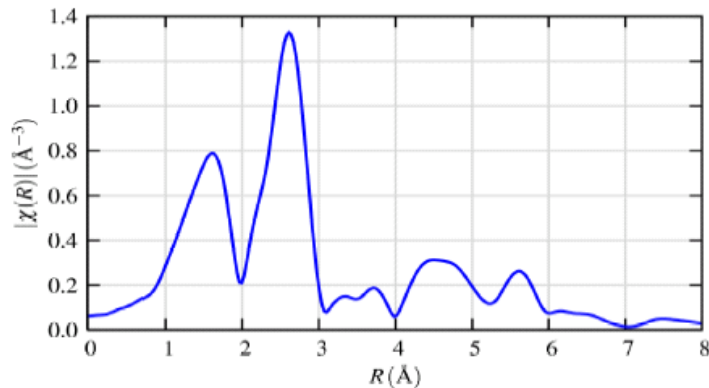
## Pre-edge:

- localized electronic states
- coordination chemistry



## XANES: (DOS)

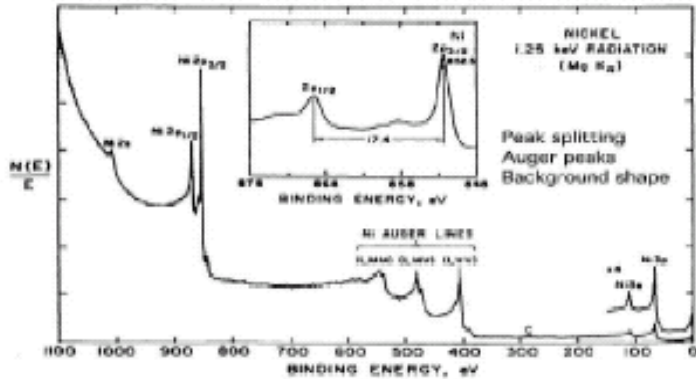
- oxidation state
- band structure
- multiple scattering



## EXAFS:

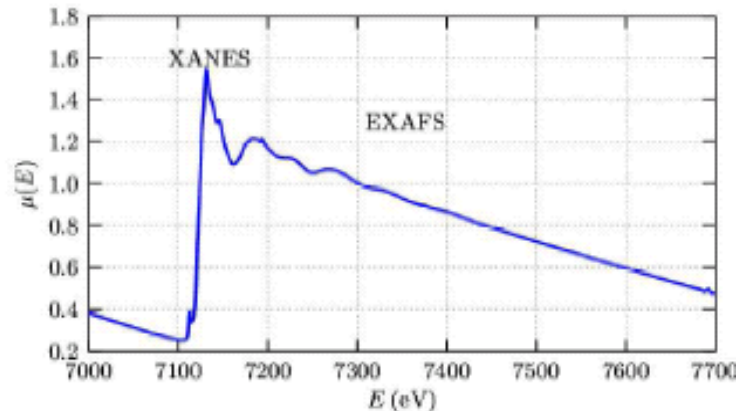
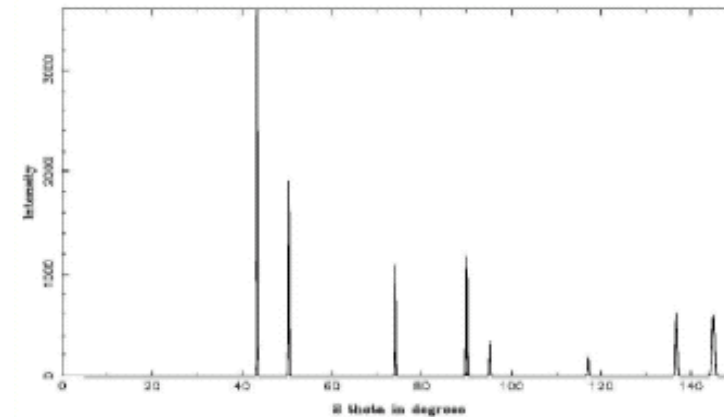
- Identity of nearest neighbors
- Bond distances
- Coordination numbers
- Amount of disorder

# Comparison: XPS, XRD, XAS



- electronic information
- surface sensitive
- In-situ application difficult
- UHV needed

- structural information
- bulk technique
- In-situ
- long range order



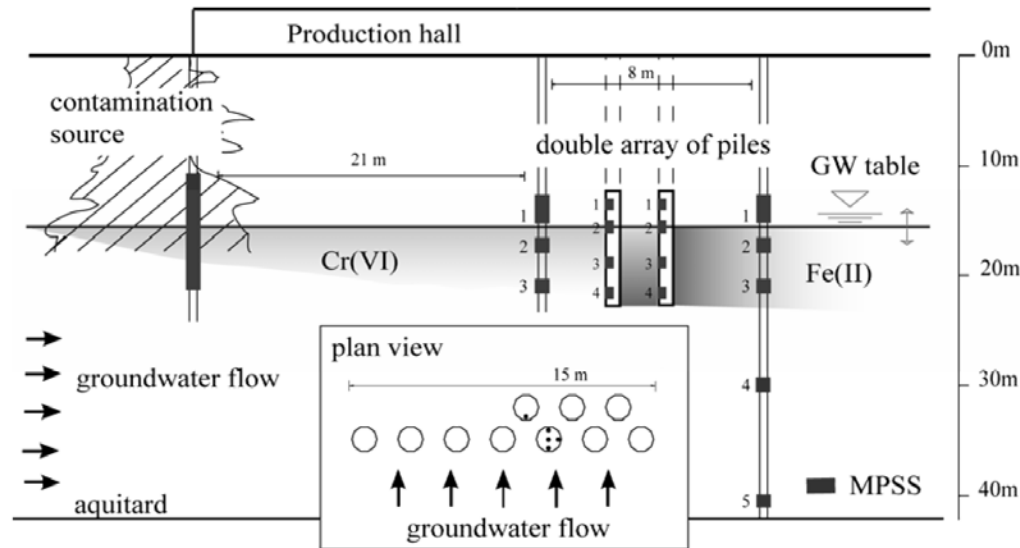
- electronic and structural information
- bulk and surface sensitive
- amorphous materials
- In-situ
- synchrotron needed



---

# Example: Fe-oxides as contaminant sorbent

---



$E_H = 150 \text{ mV}$   
 $[\text{SO}_4^{2-}] = 30 \text{ mg/L}$   
 $[\text{NO}_3^-] = 11 \text{ mg/L}$   
 $\text{pH} = 7$

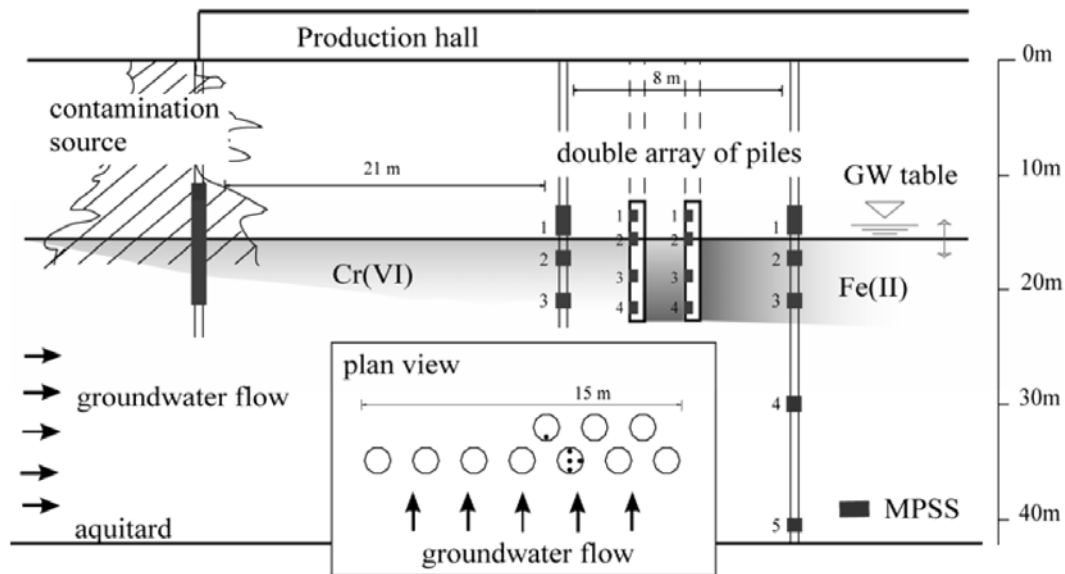


- Contaminants Cr(VI), Cu
- ~1 t Cr at a depth of 3-12 m
- Groundwater protection zone  
 $[\text{Cr(VI)}]_{\text{max}} = 0.01 \text{ mg/L}$



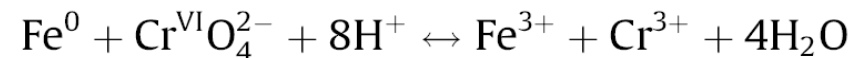
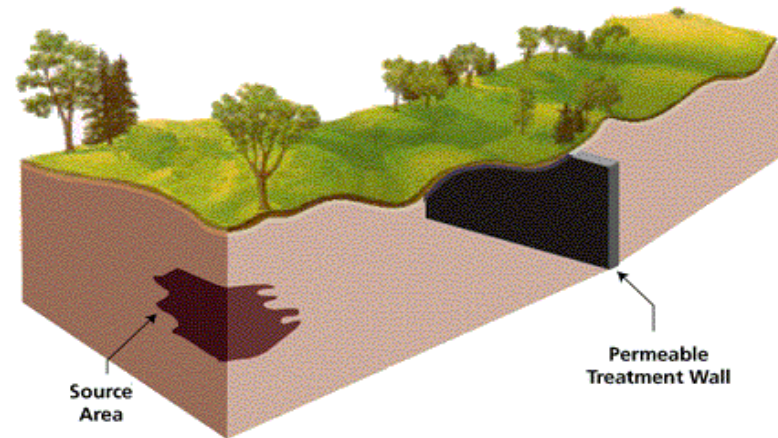
# Permeable reactive barrier

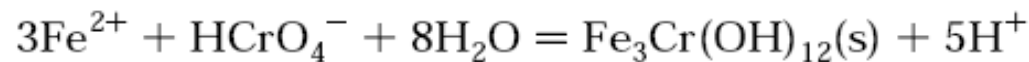
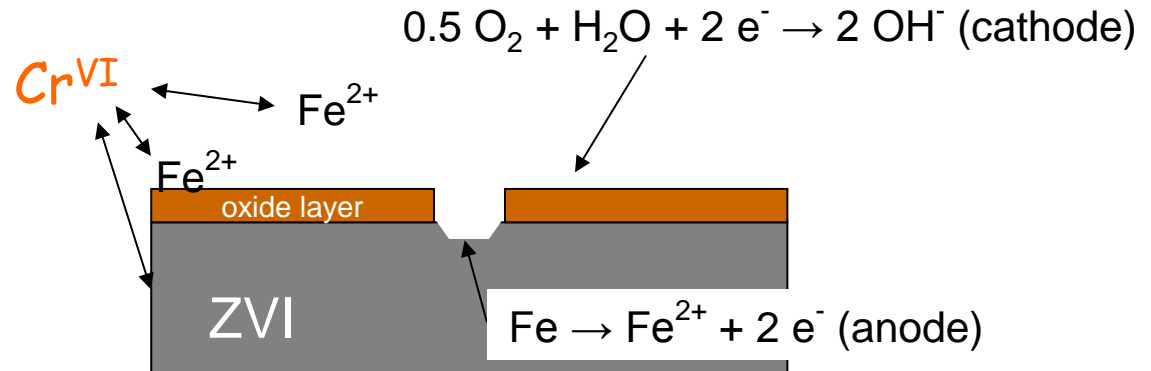
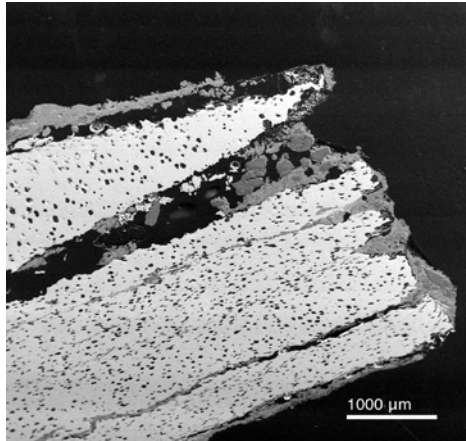
24  
Cr  
52.00



- Contaminants Cr(VI), Cu
- ~1 t Cr at a depth of 3-12 m
- Groundwater protection zone ([Cr(VI)]<sub>max</sub> = 0.01 mg/L)

Permeable Reactive Barrier (PRB):  
couple the oxidation of Fe(0) with  
the reduction of Cr(VI)





- homogeneous redox reaction (Buerge & Hug, 1997)
- heterogeneous redox reaction (Buerge & Hug, 1999)
- ZVI-Cr<sup>VI</sup>-direct reaction (Liu et al., 2008)

Molecular Cr/Fe ratio:

1/3

Hansel et al., 2003

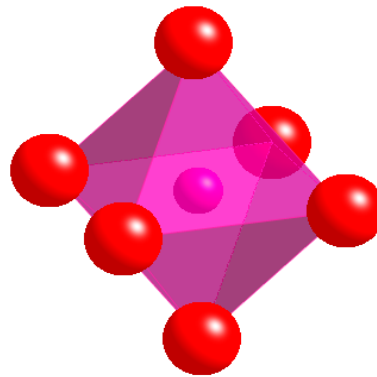
>1/3 (Cr clusters)

Grolimund et al., 1999

?

Local structure ↔ Mechanism

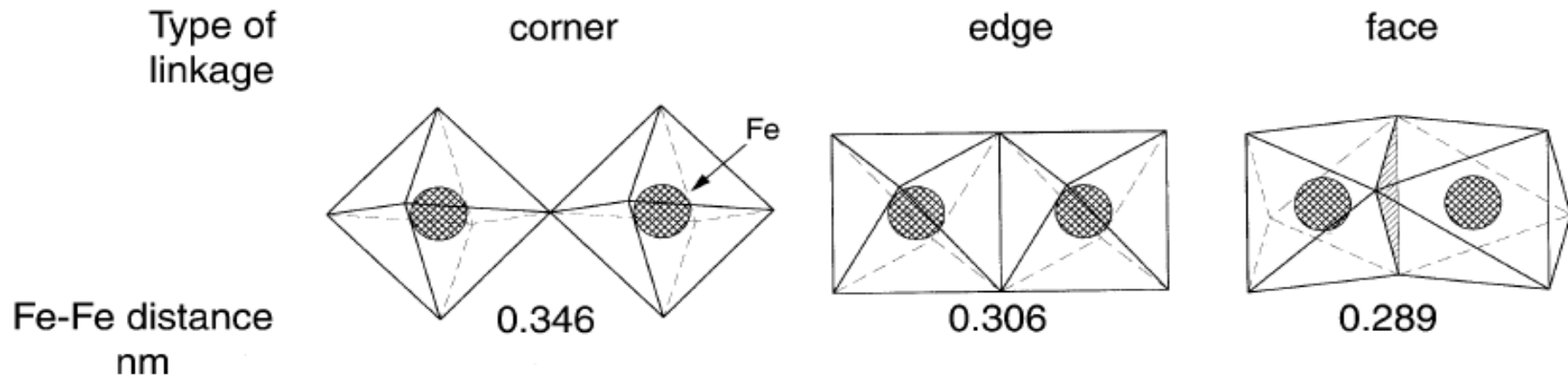
The basic structural unit  
of  $\text{Fe}^{\text{III}}$  and oxides:



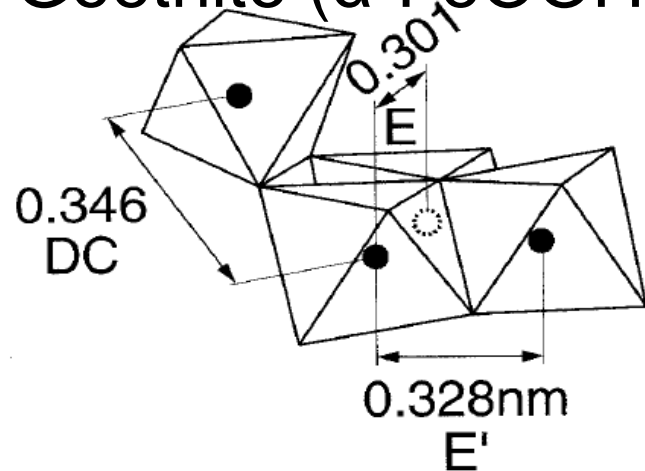
$\text{FeO}_6$  octahedron  
(also:  $\text{CrO}_3(\text{OH})_3$   $\text{FeO}_3(\text{OH})_3$ )

---

# Local structure



## Goethite ( $\alpha$ -FeOOH)



- interatomic distances
- 3D-arrangement

# Why study local (~5Å) structure ?

Nucleation, growth, aggregation of mineral phases

Sorption complexes

Important properties e.g. color  
( $\alpha\text{-Cr}_2\text{O}_3 - \alpha\text{-Al}_2\text{O}_3:\text{Cr}^{3+}$ )

Relation to molecular Fe/Cr  
(-> mechanism)

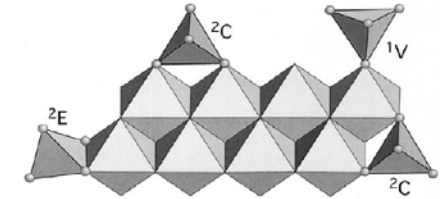
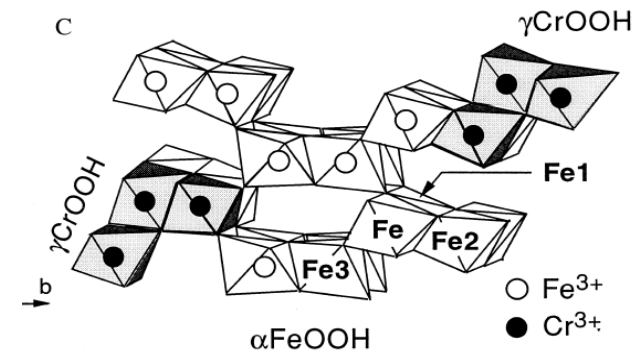
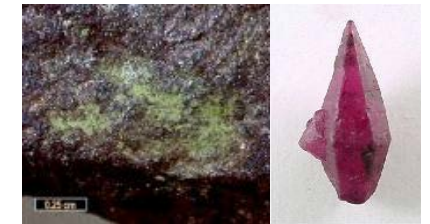
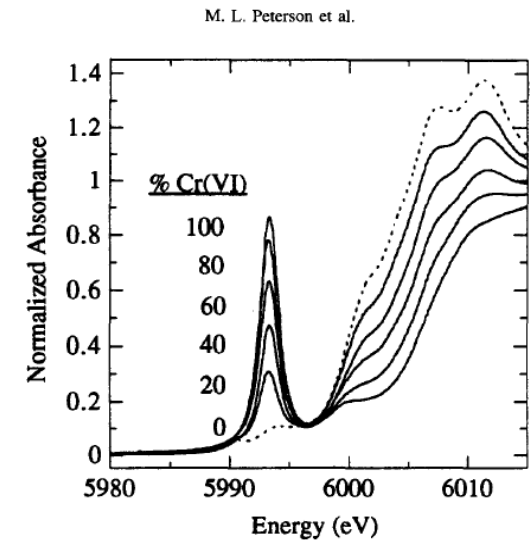
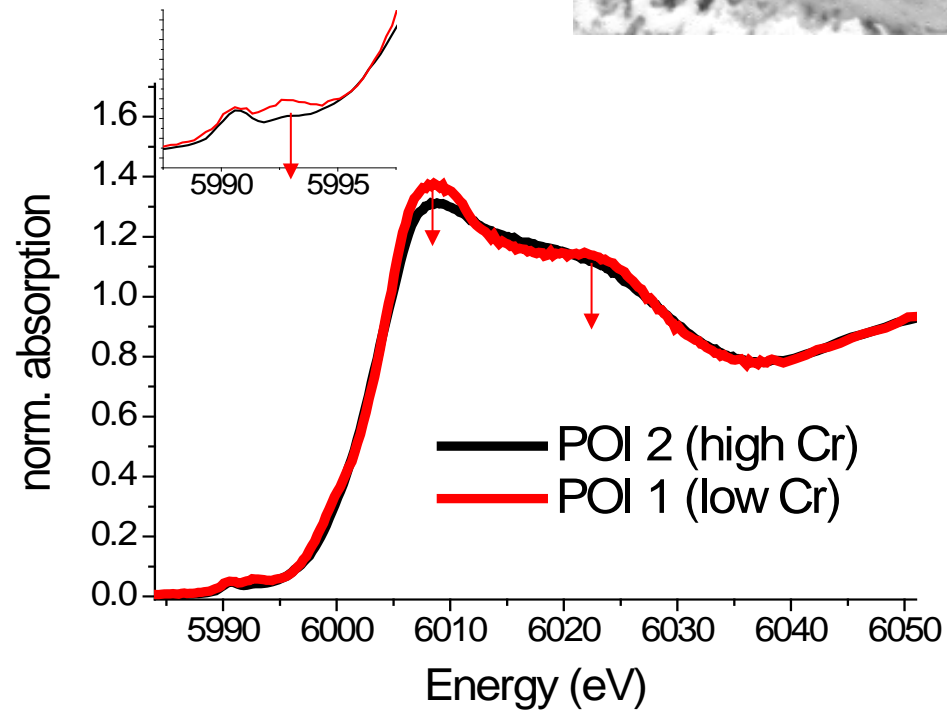
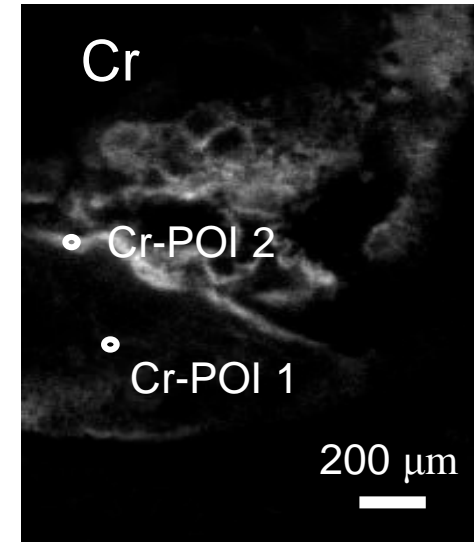
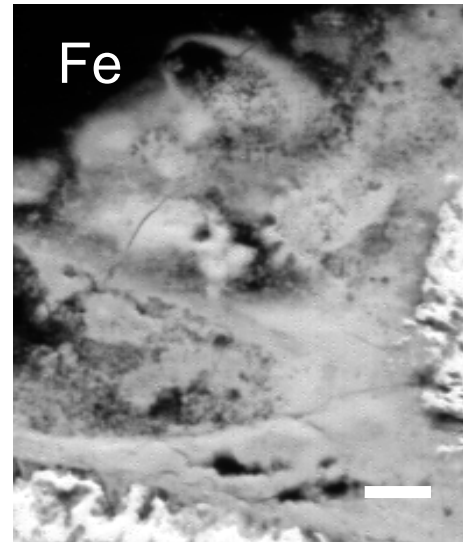
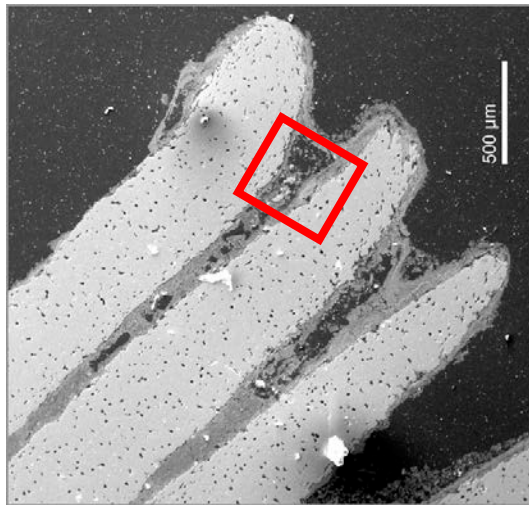


Fig. 1. Possible surface complexes of  $\text{AsO}_4$  tetrahedra on goethite.

Sherman & Randall, GCA, 67 (2003), 4223.



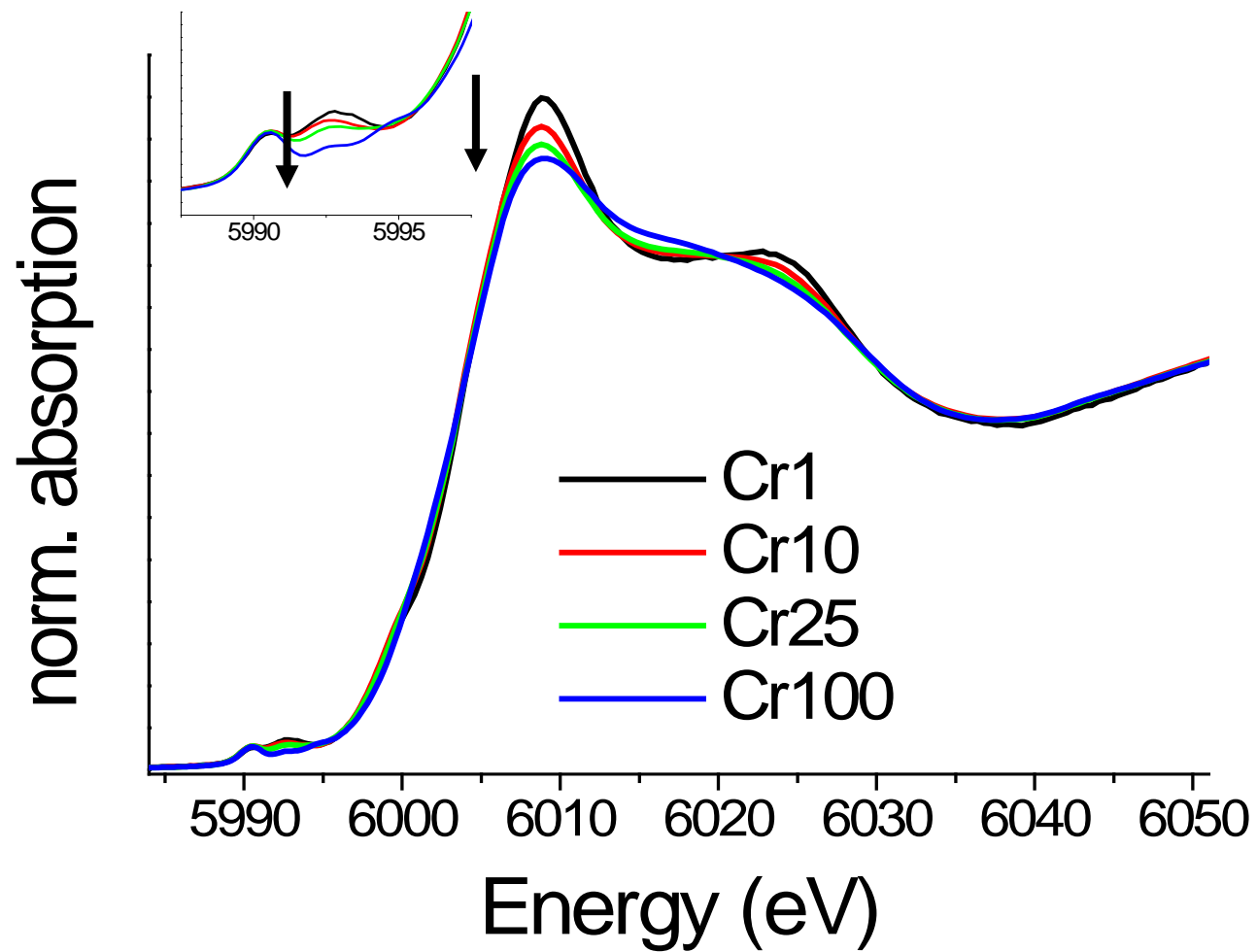
# Permeable reactive barrier

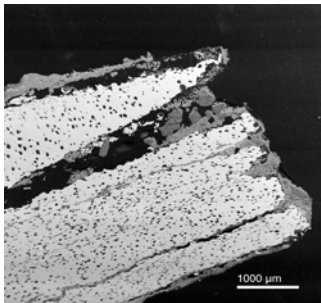


Peterson et al., *GCA* 61: 3399, 1997.

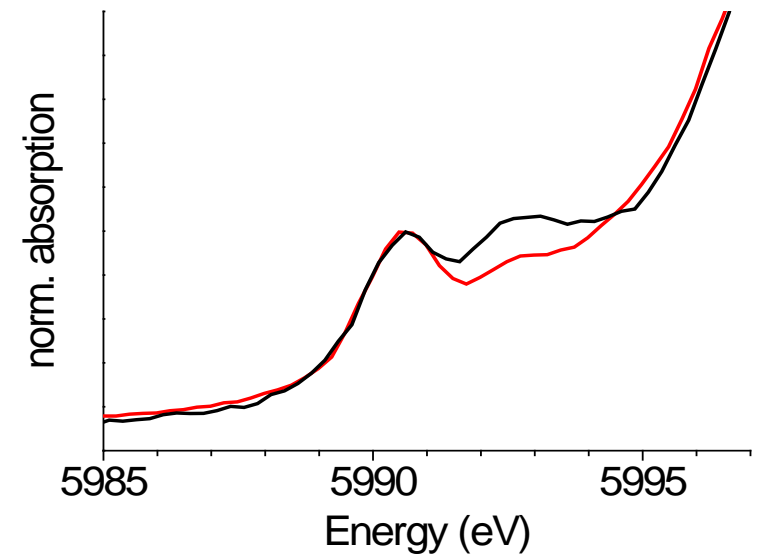
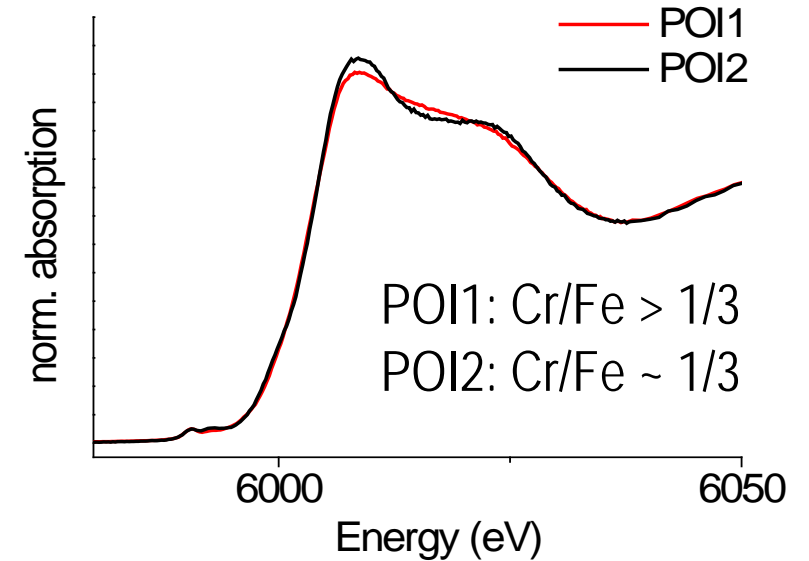
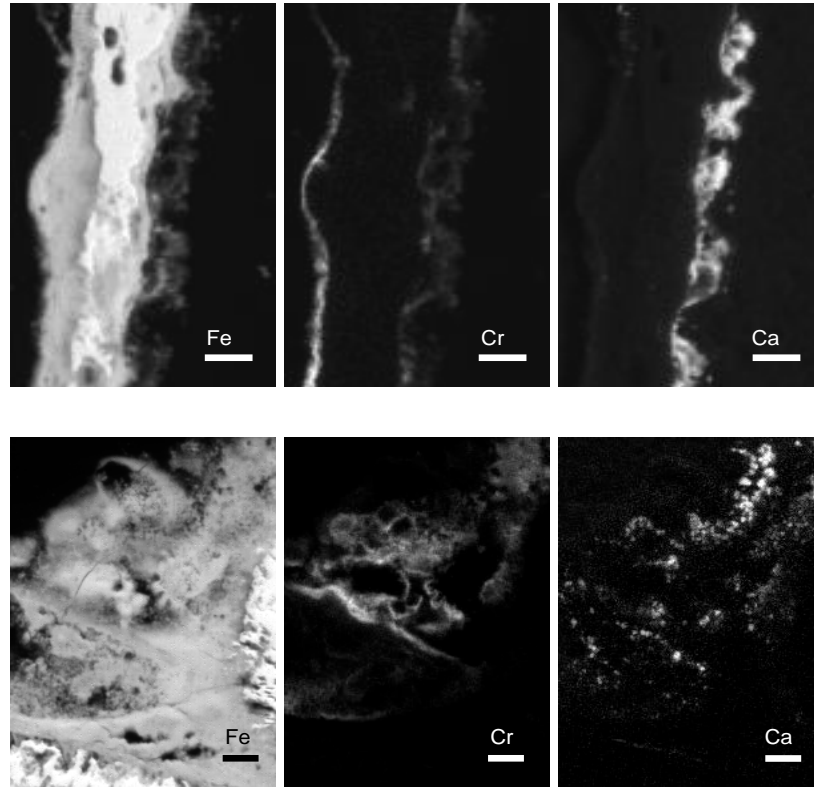


## XANES





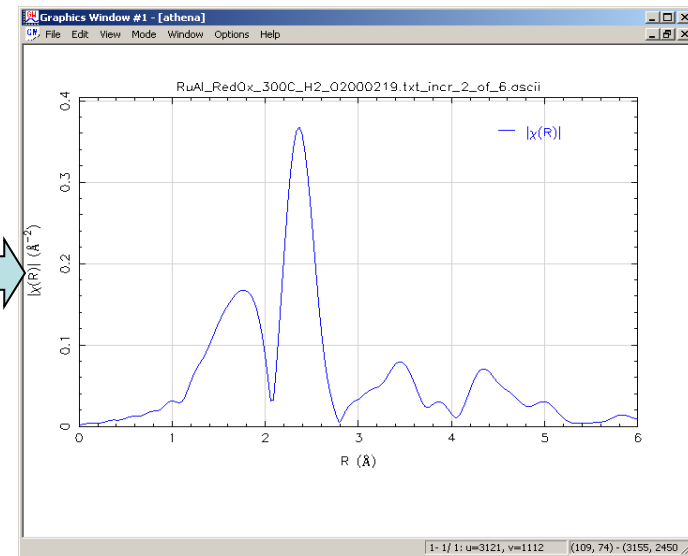
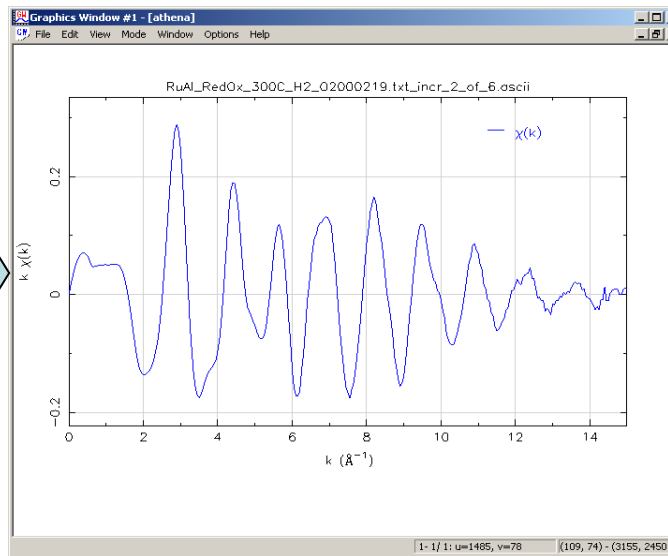
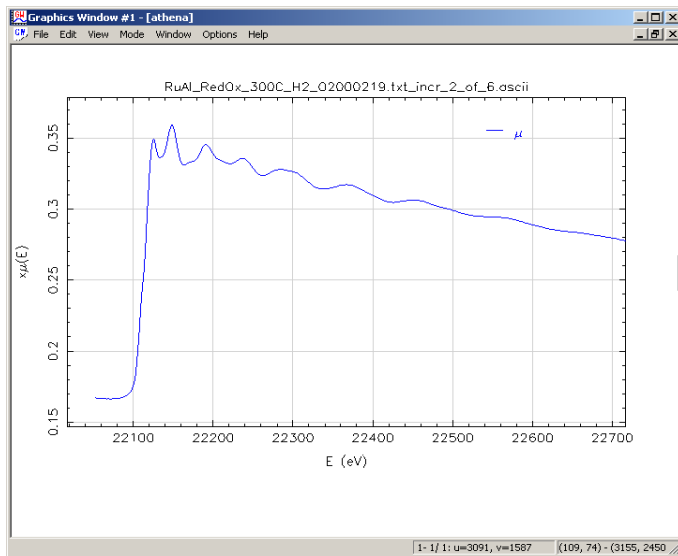
Cr/Fe < 1/10



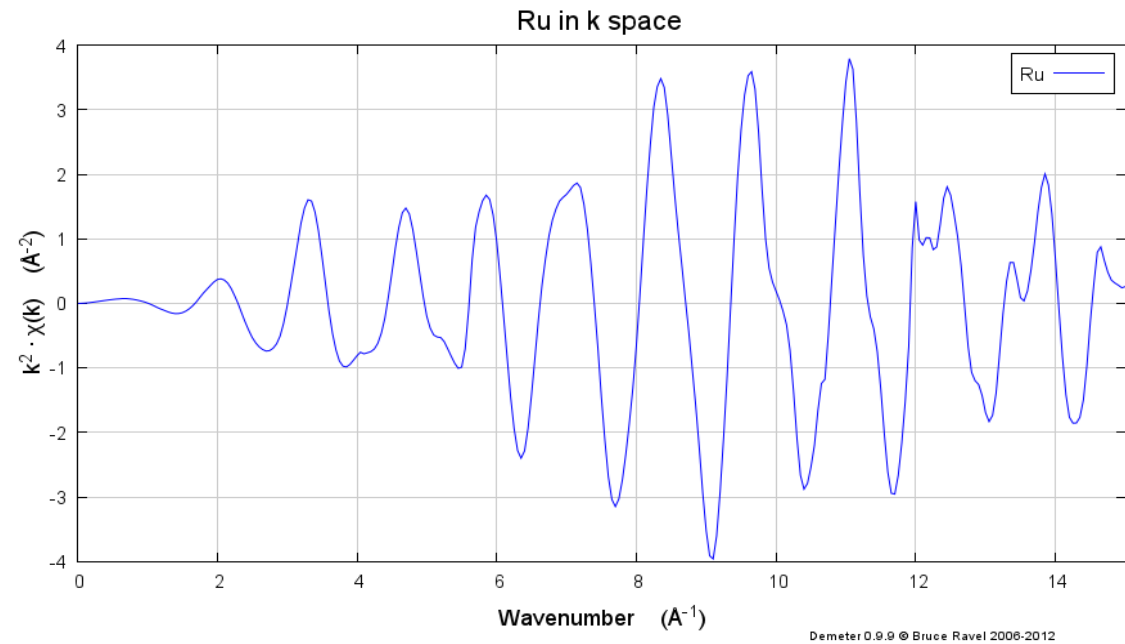
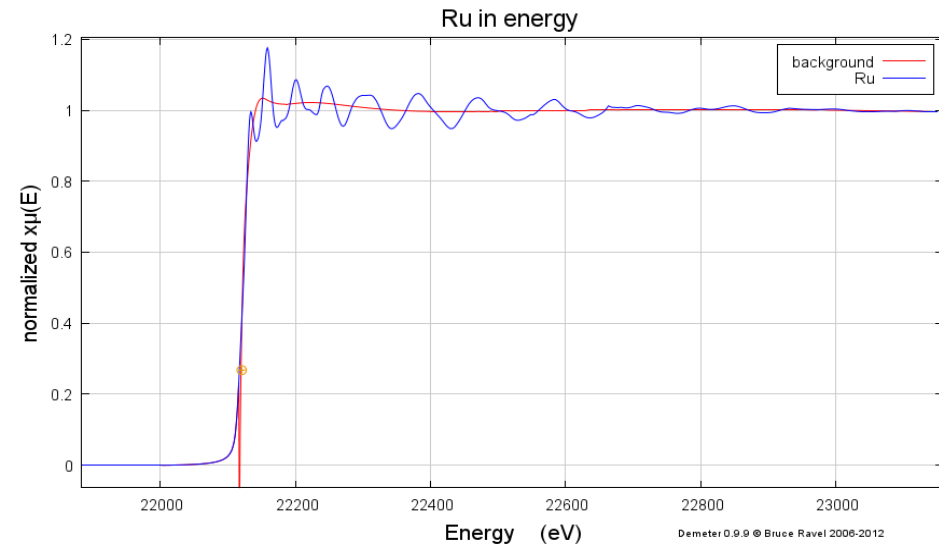
homogeneous & heterogeneous  
redox reactions

## Basic data reduction steps of

- compare data that is measured in different modes (trans. / fluo.) and correct for different absorbances
- extract the EXAFS signal ( $\chi(k)$ ) and the Fourier-transformed EXAFS signal
- look at radial distribution function, and fit the first shell neighbour



# Extraction of the EXAFS signal – $\chi(k)$



## 1. Extract EXAFS signal

- Subtract smooth background

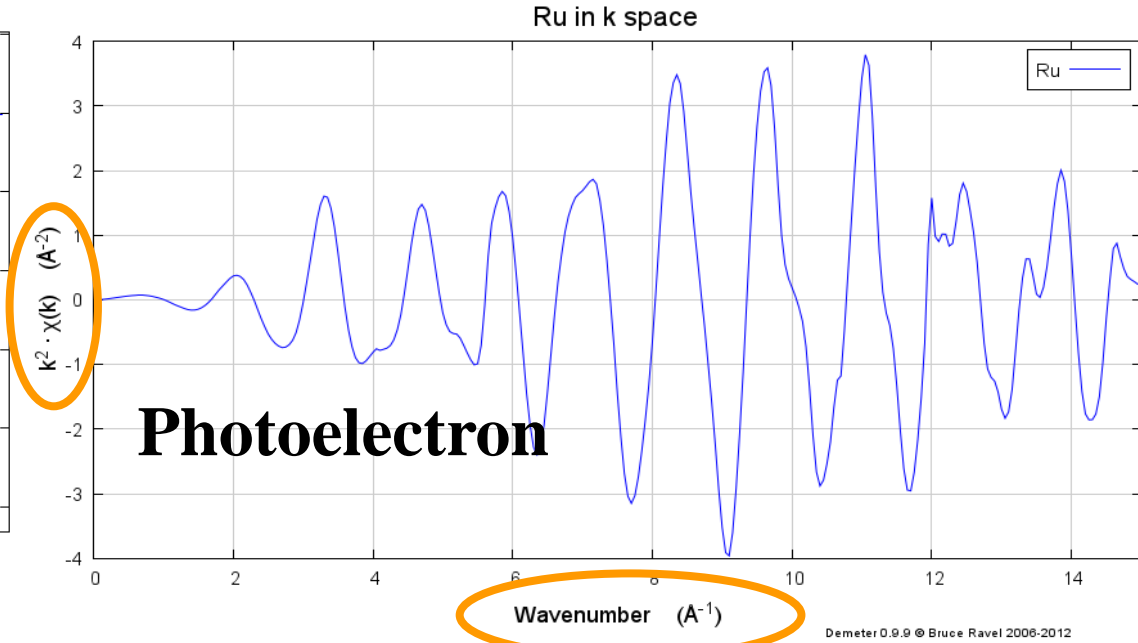
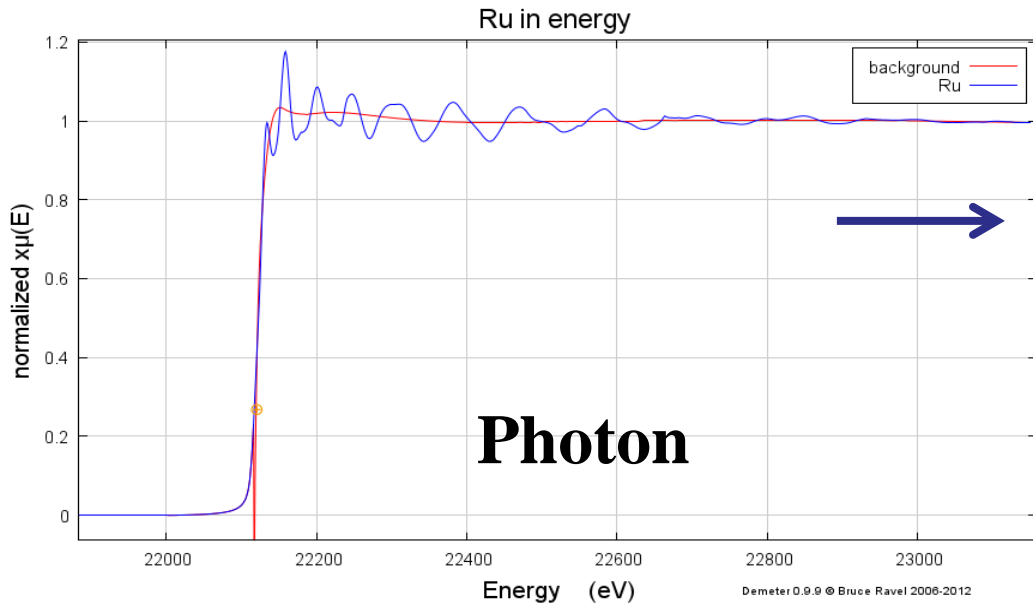
Normalized oscillatory part of absorption coefficient

Measured Absorption coefficient

Bkg: Absorption coefficient without contribution from neighboring atoms (Calculated)

$$\chi(E) = \frac{\mu(E) - \mu_0(E)}{\Delta\mu(E)} \sim \frac{\mu(E) - \mu_0(E)}{\Delta\mu(E_0)}$$

Evaluated at the Edge step ( $E_0$ )



## 2. Transformation from E-space to k-space

- Scattering of photoelectron on neighboring atoms
- Unit of k-space: inverse Angstroms
- „stretch“ the x-axis
- amplify signal at high energies (k-weight)

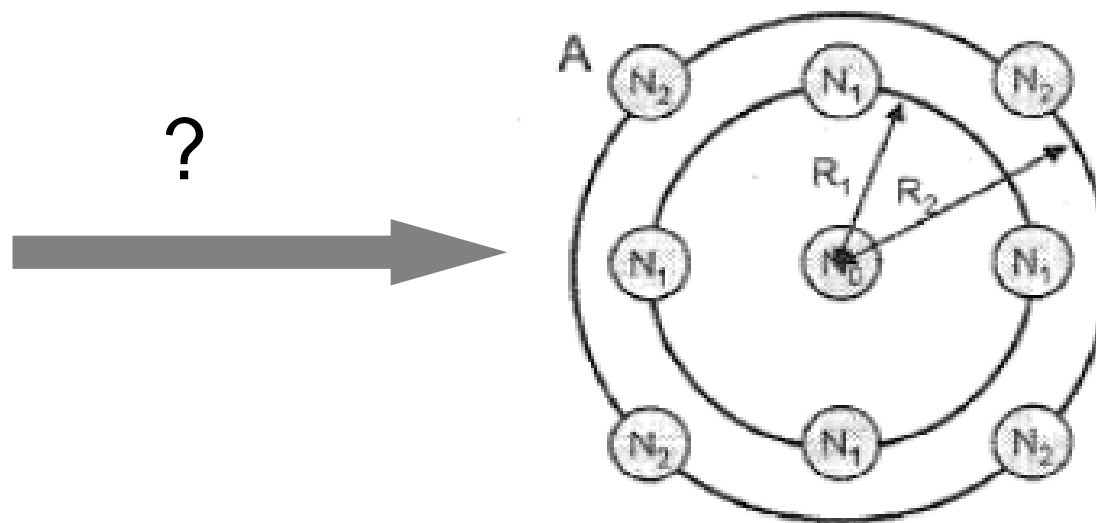
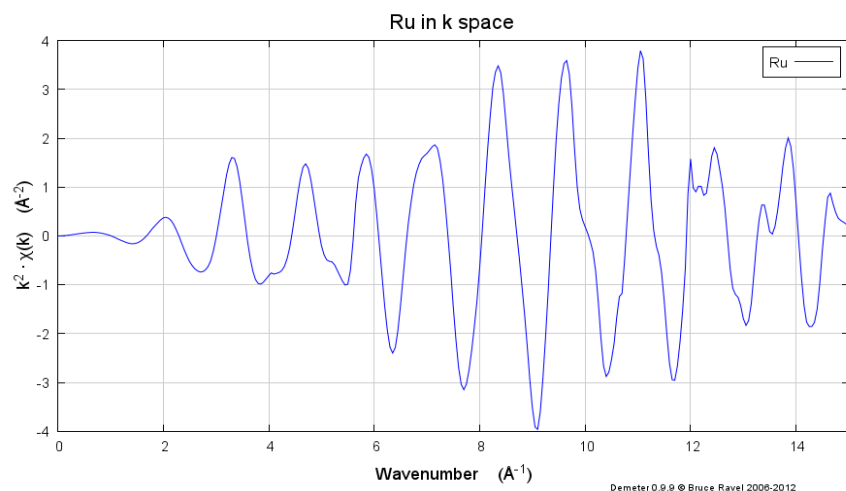
$$k^2 = \frac{2m_e(E - E_0)}{\hbar^2} \sim \frac{\Delta E}{3.81}$$

Mass of electron

Edge Energy

Plank's constant

To understand and visualize the geometric structure of our sample we need to Fourier transform the EXAFS signal from inverse distance into the distance domain



$N_0$  X-ray absorbing atom

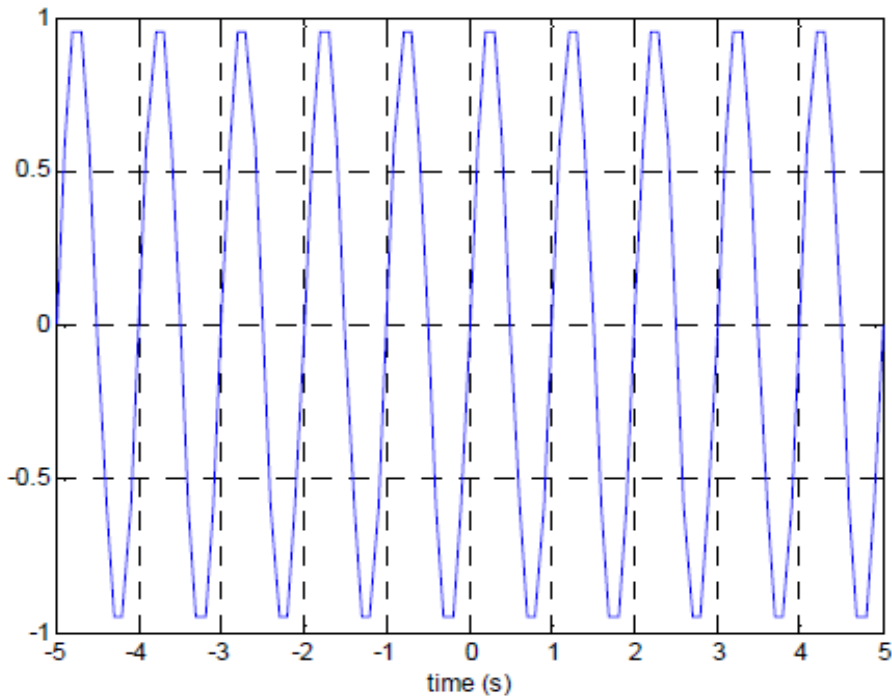
$N_1$  1<sup>st</sup> neighboring scatterer (shell)

$N_2$  2<sup>nd</sup> neighboring scatterer (shell)

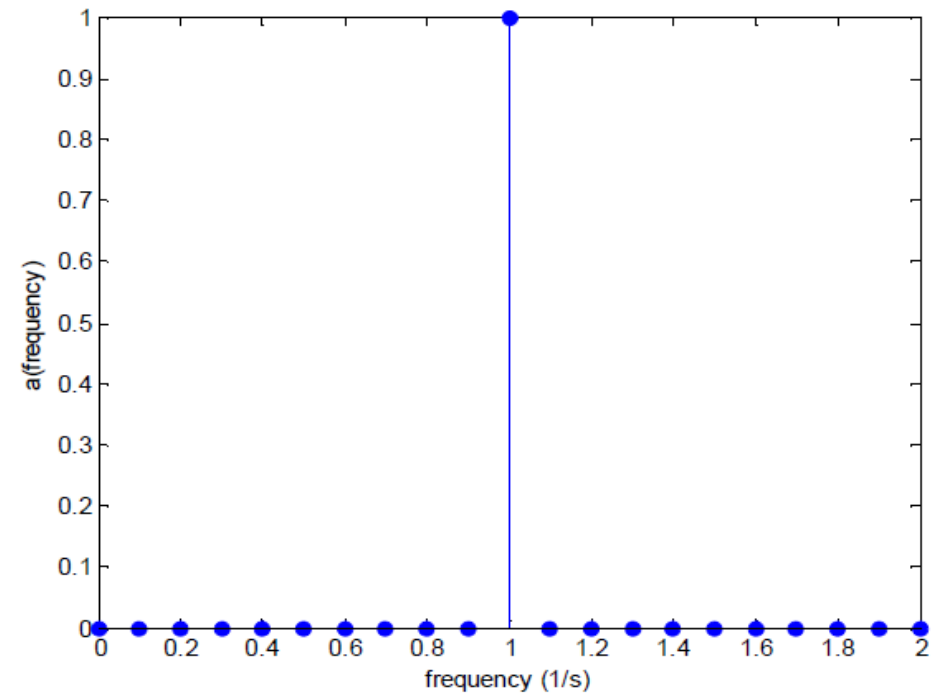
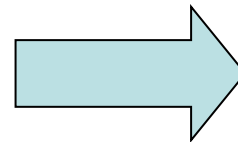
$R_x$  distance between absorber and scatterer

# Fourier transformation crash course

- FT transforms data from one dimension into its reciprocal one
- example: transformation from the time into the frequency domain



Wave function with period length of 1 s



Frequency of 1 Hz

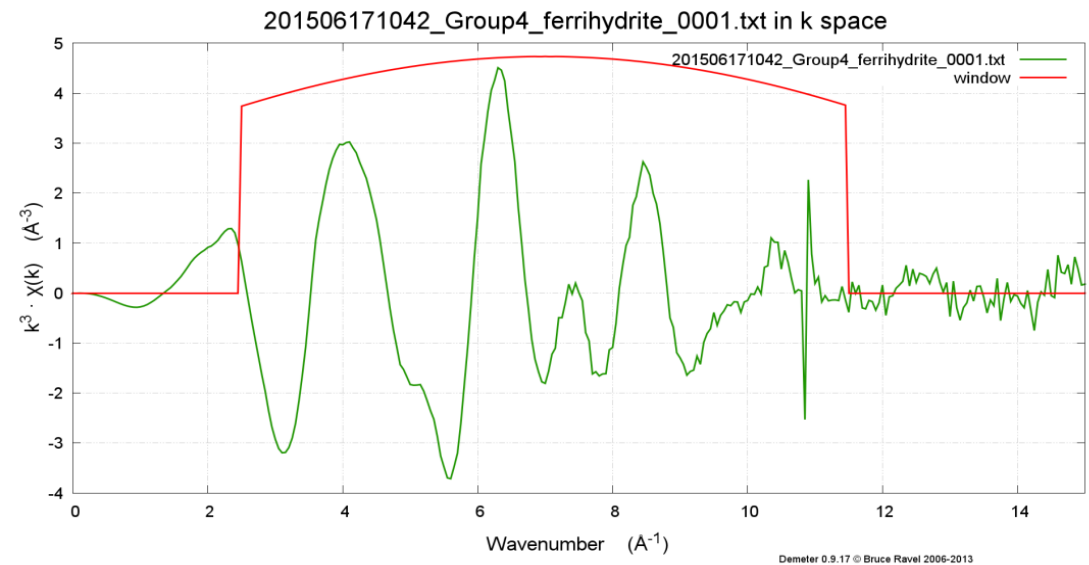
## Define k-range for Fourier transformation

Lower limit: 2-3  $\text{\AA}^{-1}$  ; upper limit: as far as reasonable (consider signal to noise)

**Fourier Transform Button**

**Forward Fourier transform parameters**  
 k-range 2.000 to 13.211 dk 1 window Hanning  
 arbitrary k-weight 0.5 phase correction

**Plot in k-space**  
 x(E)  Window



**Recover the distance of scattering atoms from the frequency of the scattered wave**

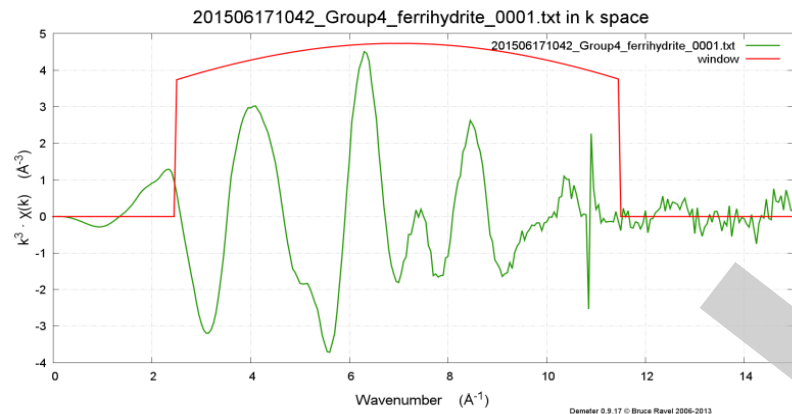
→ Fourier transform the EXAFS function (from  $\text{\AA}^{-1}$  to  $\text{\AA}$ )



Fourier transformed of the EXAFS signal

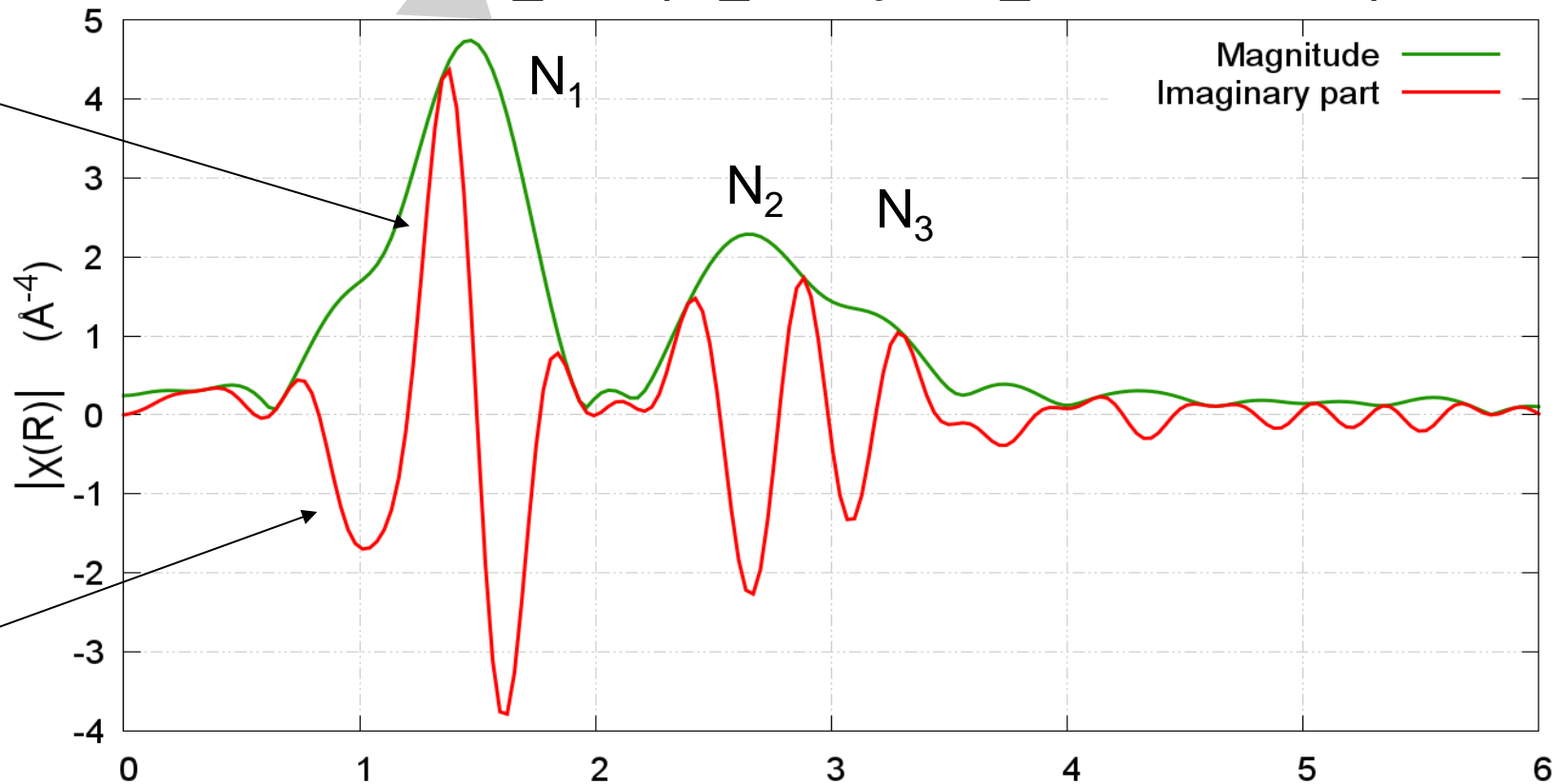
Remember: FT creates a complex function

→ always show magnitude AND real or imaginary part



201506171042\_Group4\_ferrihydrite\_0001.txt in R space

magnitude

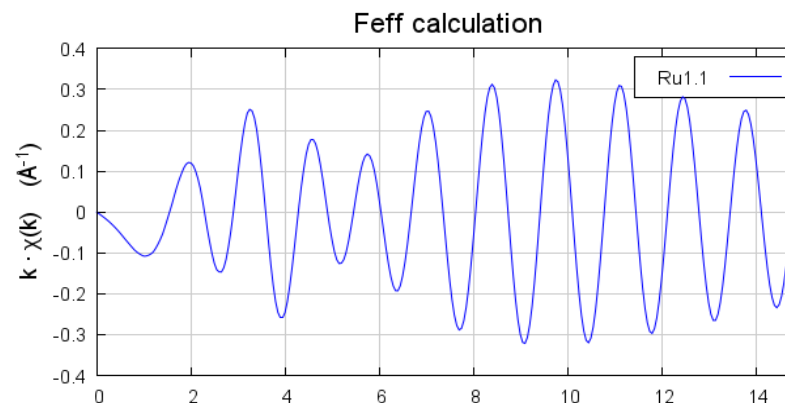
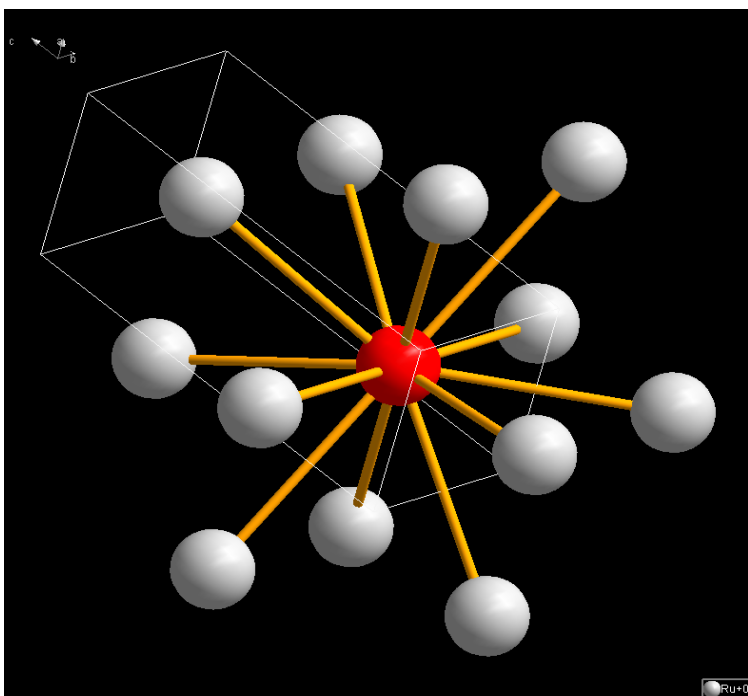


Imag part

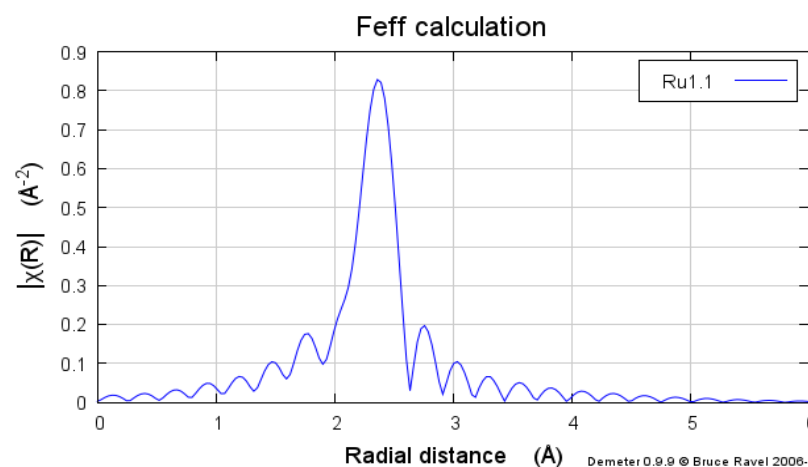
Radial distance (Å)

The pseudo RDF created in the previous step is now analyzed by fitting with a set of model structures

- ➔ Create a model of the assumed structure
- ➔ Calculate the EXAFS function of this theoretical structure (ATOMS @ ifeffit)
- ➔ Fit the model to the data, extract structural parameters



Calculated  
scattered  
wave



Corresponding  
RDF

What information can we extract from a fit?

EXAFS function

$$\chi(k) = \sum_i \frac{N_i F_i(k) S_0^2}{k R_i^2} e^{-\frac{2R_i}{\lambda}} e^{-2\sigma_i^2 k^2} \sin(2kR_i + \phi_i(k))$$

Sum of damped sine functions with a pre-factor

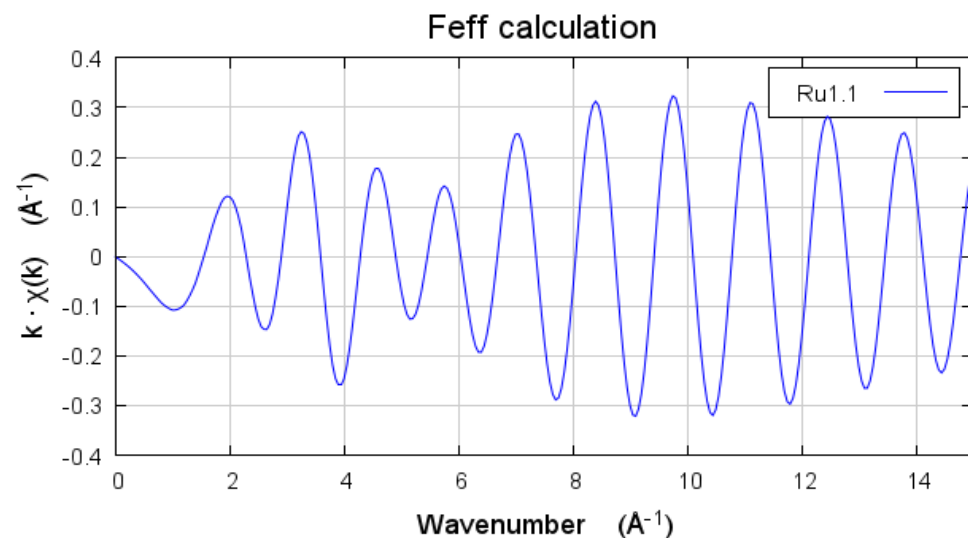
Structural Parameters:

N: coordination number → amplitude

R: radial distance → frequency

$\sigma^2$ : pseudo Debye waller factor → damping

Theoretical first Ru-Ru shell of metallic ruthenium

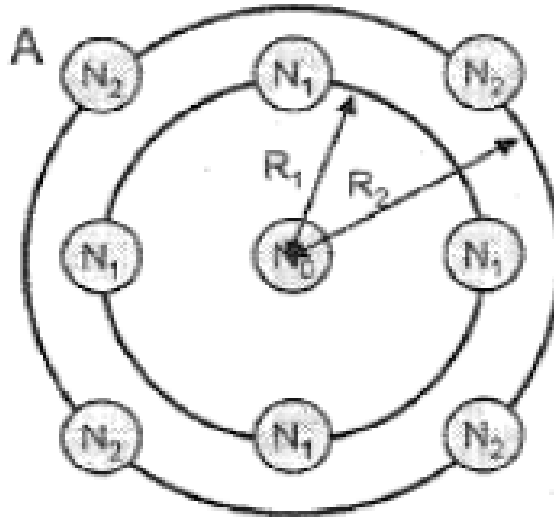


Demeter 0.9.9 © Bruce Ravel 2006-2012

**Calculate EXAFS signal of model compound! → FEFF**

Reminder: what's a coordination shell?

Every shell of atoms has a specific distance from the absorber and a specific coordination number



From fitting of EXAFS data information about

- the distance  $R$  of each shell from the absorbing atom
- the number of atoms in each shell (coordination number) is obtained.

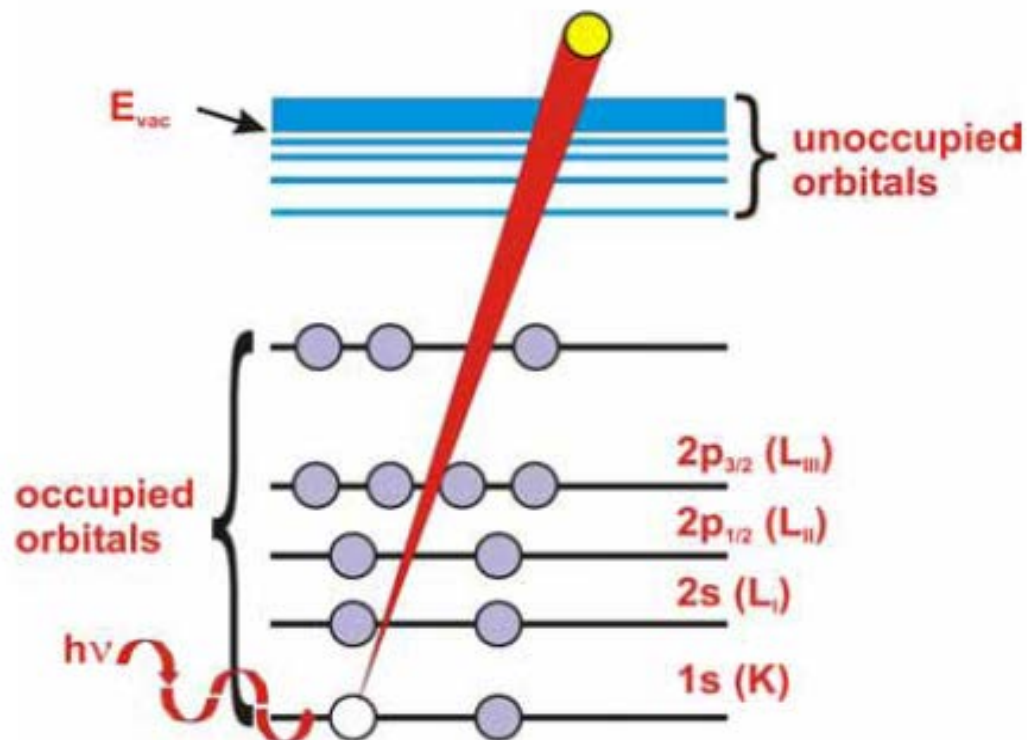
Beamline	Energy Range (keV)	Spot Size ( $\mu\text{m}$ )	K-Edges	Absorption	Fluorescence	Electron yield	Speciality
PHOENIX	0.8 - 8	2 x 2	Na - Co	x	x	x	Energy Range Variable Polarization
MicroXAS	5 - 23	1 x 1	Ti - Mo	x	x		Femto Diffraction radioactive samples
SuperXAS	6 - 40	5 x 10	Cr - La	x	x		Absorption, Fluorescence, Quick, Chemical environments
Pollux	0.2 - 1.2	0.04 x 0.04	C - Mg	x	(x)		Nano focus, STXM, absorption spectroscopy, phase contrast
nanoXAs	0.2 - 1.2	0.04 x 0.04	C - Mg	??	??	x	Combine AFM with STXM



Thank you for your attention! Questions?

---

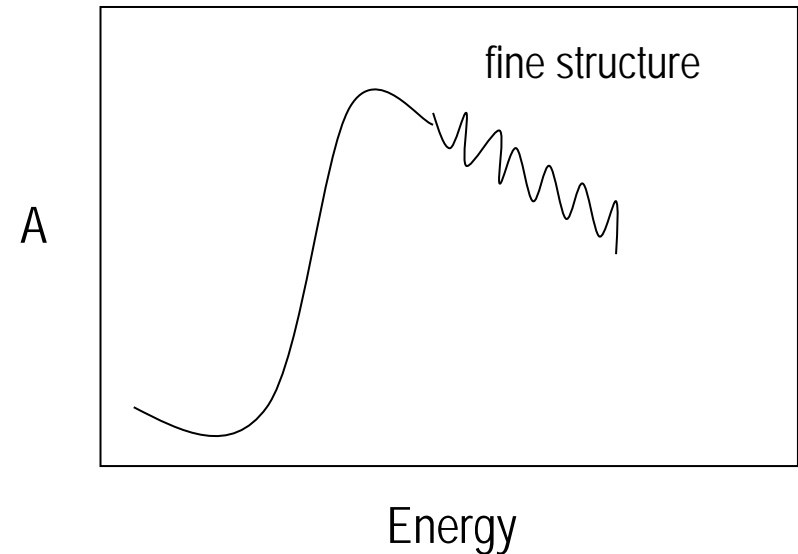
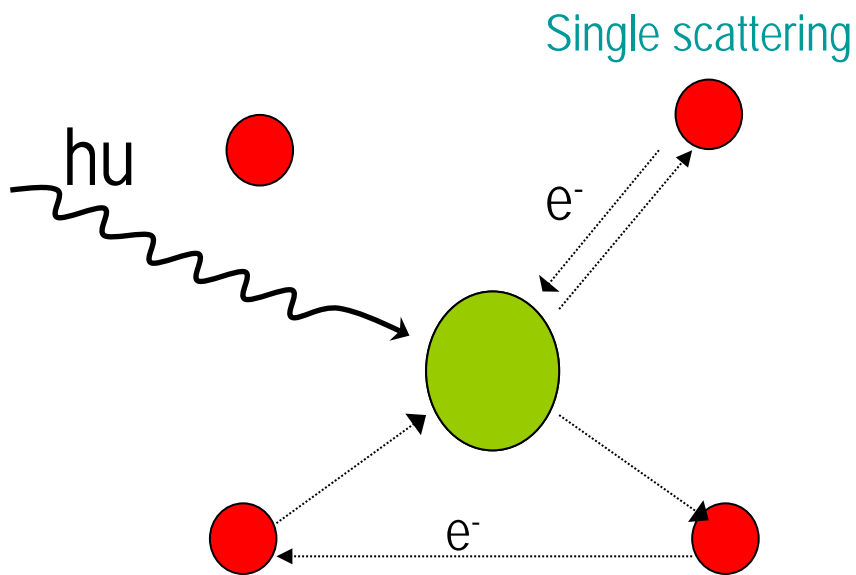
# The basic concept of XAFS



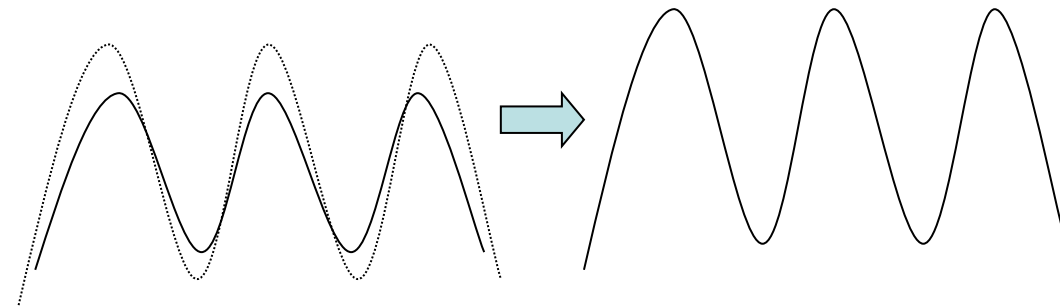
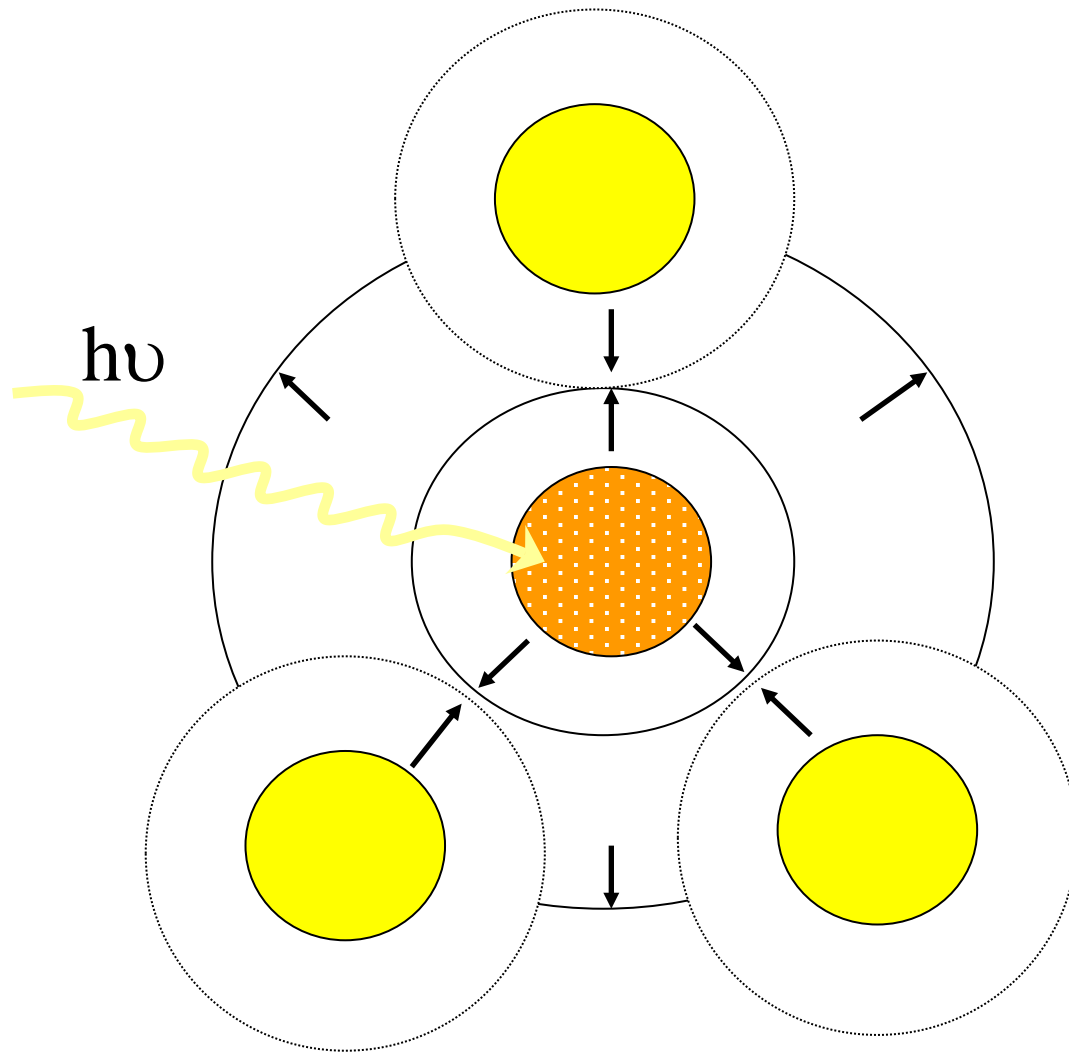
X-rays (light with wavelength 0.06- 12 Å or energy 1-200 keV) are absorbed by all matter through the **photo-electric effect**:

An X-ray is absorbed by an atom when the energy of the X-ray is transferred to a core level electron (K, L, or M shell) which is subsequently ejected from the atom. Any excess energy from the X-ray is given to the ejected photo-electron.

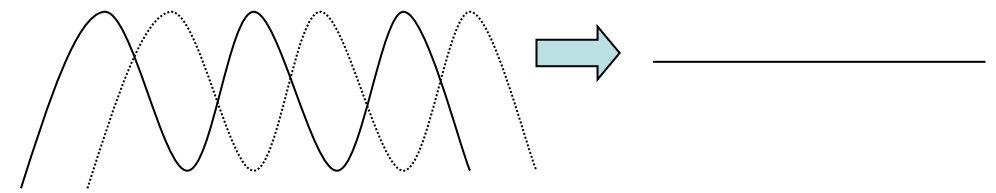
Electrons have a particle and wave nature. The photoelectron wave propagates away from the central atom (absorber), and it may scatter off neighboring atoms and finally return to its point of origin.







In phase



Out of phase

The consequence of these scattering phenomena and wave interactions is that the intensity of X-ray absorption oscillate with a dependence on the structural environment of the absorber. Mathematically modeling these oscillations provides precise local structural information.